https://doi.org/10.5194/egusphere-2026-3582
Preprint. Discussion started: 10 July 2026

Do the same river engineering works cause the same morphological adjustments? Context matters!

Gabrielle Seignemartin[1, 3], Brice Mourier[1], Jérémie Riquier[2], Hervé Piégay[3]

1. Univ. Lyon, Université Claude Bernard Lyon 1, CNRS, ENTPE, UMR5023 LEHNA, F-69518, Vaulx-en-Velin, France
2. Univ. Jean Monnet Saint-Étienne, CNRS, UMR 5600 – Environnement-Ville-Société, F-42023, Saint-Étienne, France
3. Univ. Lyon, ENS de Lyon, CNRS, UMR 5600 EVS, 69362 Lyon Cedex, France

Correspondence to: Gabrielle Seignemartin (gabrielle.seignemartin@gmail.com)

Abstract. Rivers in the Anthropocene have undergone significant geomorphological changes due to engineering interventions such as channelization and hydroelectric infrastructure. These modifications have disrupted hydrological and sedimentary processes, reducing hydrological connectivity and habitat diversity. Evaluating their impacts is crucial for river management and restoration. We studied four channelized and bypassed sections of the French Rhône River (>60 km; ~13% of its length). We analyzed spatio-temporal trajectories of channel narrowing and margin terrestrialization using GIS-based analysis of historical maps, aerial photographs, and satellite imagery. Historical hydrosedimentary data, including longitudinal profiles and water-level records, were used to assess the contribution of successive development phases. Beyond qualitative observations, such as the simplification of the river pattern toward a single-thread channel, we quantified the variable contributions of channelization and flow diversion. Active-channel narrowing ranged from −43% to −17% following channelization and from −32% to −17% following flow diversion. Margin terrestrialization increased by 27–44% and 41–66%, respectively. Where channelization had limited effects on terrestrialization, flow diversion played a greater role via water-level changes and reshaping the alluvial mosaic dependent on hydrological gradients. Although bed incision is generally expected to be limited in bypassed reaches, it reached −4.1 m in the most affected section (−5 $cm \cdot y^{-1}$ during the 20th century), largely due to gravel mining associated with dam construction. This four-site comparison displays that engineering pressures interacted with local hydrosedimentary conditions to produce contrasting, legacy-dependent trajectories. Engineering margins, as ecotonal zones, are key indicators of geomorphic adjustment, documenting the system's response to successive development phases.

1. Introduction

Over the past two centuries, rivers in the Anthropocene era (Crutzen and Stoermer, 2000; Crutzen and Steffen, 2003; Bonneuil and Fressoz, 2013) have undergone significant transformations due to successive engineering phases, including flood control infrastructure, channelization, and hydroelectric development (Bravard and Petts, 1996; Gregory, 2006; Kelly et al., 2018). In large river systems under multiple pressures, it is challenging to disentangle the cumulative impacts of these pressures.

https://doi.org/10.5194/egusphere-2026-3582
Preprint. Discussion started: 10 July 2026

However, it is well established that anthropogenic influences have fundamentally altered the hydrological and sedimentary processes driving eco-morphodynamics, leading to major landscape and ecosystem changes (Petts, 1987; Dynesius and Nilsson, 1994; Nilsson and Berggren, 2000; Tockner and Stanford, 2002; Gregory, 2006). These interventions generate interrelated impacts across spatial and temporal scales, requiring a systemic approach to understand their eco-geomorphic consequences (e.g., Surian, 1999; Vázquez-Tarrío et al., 2019; Tena et al., 2020). A key challenge in this context is determining whether similar engineering interventions on rivers lead to comparable geomorphic responses.

Despite spatial and temporal variations in the sequences of river modifications, two recurrent phases across Europe provide a valuable framework for assessing geomorphic responses by type and magnitude. The first phase, which began in the 19th century, saw the widespread implementation of hydraulic infrastructures such as lateral dikes and groin fields for stabilizing and straightening the riverbed and promoting navigation (Copeland, 1983; Brooker, 1985; Brookes, 1985; Sukhodolov et al., 2002; Hudson et al., 2008). This phase is referred to hereafter as Phase 1. These engineering works induced morphological homogenization of river channels, disrupted alternate bar patterns, and contributed to riverbed degradation (e.g., Brookes, 1981; Brooker, 1985; Surian and Rinaldi, 2003; Bravard, 2010). Furthermore, lateral hydraulic structures (e.g., dikes, riprap protection, and groin fields) restricted lateral shifting and connectivity, reduced sediment supply from lateral erosion, and promoted sediment accumulation along riverbanks (Citterio and Piégay, 2009; Dépret et al., 2017; Vauclin et al., 2020a). In the 20th century, many of these watercourses were further modified for hydroelectric development (Petts, 1987; Petts and Gurnell, 2005; Belletti et al., 2020), a stage we refer to as Phase 2. Among the various impacts, dams have notably disrupted downstream bedload transport and altered flow regimes, creating imbalances between bedload transport and flow—both key variables in morphodynamics. These changes have led to bedload deficits, riverbed incision, and sediment coarsening, which can ultimately result in armoring (Williams and Wolman, 1984; Kondolf, 1997; Vörösmarty et al., 2003; Graf, 2005; Petts and Gurnell, 2005; Kondolf et al., 2014). Additionally, in these highly modified systems, gravel mining activities have imposed further pressure, often reshaping bed topography and disrupting sediment transport processes (Petit et al., 1996; Kondolf, 1997; Brunier et al., 2014).

Rivers with both channelized and bypassed sections, such as the Rhône, Danube, and Rhine rivers—once characterized by multi-thread or anabranching systems—have largely transitioned into single-thread channel configurations (Hohensinner et al., 2004; Arnaud et al., 2019). With 12 bypasses between Lyon and the Mediterranean Sea, the bypassed sections of the Rhône River in France span more than 120 km, representing approximately 22% of the total length of its French course (~545 km) and 35% of its course downstream of Lyon. This estimate excludes the impacts of dam reservoirs and upstream backwater zones. Thus, the Rhône provides a unique natural laboratory for examining these transformations, offering comparable study sites and a distinctive vantage point owing to its distinctive dike systems. A defining feature of its regulation is the presence of unique structures, including not only classical groin fields but also the distinctive casier Girardon—hydraulic units named after their designer, composed of oblique backing dikes supporting a longitudinal submersible dike. Since their construction in the late 19th century to enable year-round navigation, these structures have influenced the river morphological evolution, serving both as records of past anthropogenic pressures and as valuable sedimentary archives, exemplifying the legacy sediment concept (Vauclin et al., 2020b).

In assessing the geomorphic evolution of dike fields throughout the 20th century in a reach of the middle Rhône River (Péage-de-Roussillon), we identified two main processes driving terrestrialization—the transformation of aquatic areas into terrestrial ones (Seignemartin et al., 2023). The first process involves marginal deposition and accumulation of fine sediments, which occurs as a result of the presence of dike fields (Phase 1) that create areas with reduced shear stress. The second process, which leads to the formation of terrestrial surfaces, is linked to the lowering of water levels. This can be driven by either riverbed incision triggered by channelization (Phase 1) or the reduction of water discharge caused by diversion (Phase 2). In the Péage-de-Roussillon reach, up to 70% of terrestrialized in-dike surfaces can be linked to the water level drop following dam construction. Although the same types of river engineering modifications were applied across the Rhône, the timing of their implementation—particularly that of diversion schemes—often differed. The specific geomorphological and infrastructural features of each reach raise the question of whether similar in-dike terrestrialization processes occurred in other channelized or bypassed sections. Despite their prevalence, these processes remain insufficiently studied in isolation. Although some studies examine the cumulative impact of anthropogenic pressures (e.g., Tena et al., 2020), few inter-site provide a detailed, phase-specific quantitative evaluation.

This framework allows us to address the following key scientific questions: Have channelized and bypassed reaches undergone similar geomorphic adjustments? How does terrestrialization manifest in engineered alluvial margins, and how do these margins evolve in relation to the channel and floodplain? In the present study, we aimed to compare the trajectories of alluvial terrestrialization and river responses to two phases of engineering interventions across four Rhône reaches—channelized and bypassed—that together represent one-third of the bypassed river length. These reaches are particularly suitable for investigation as they serve as pilot sites for ongoing restoration efforts. The objectives of the study are as follows:

(i) To assess the evolution of the main channel and floodplain side channels and evaluate the influence of engineering interventions on waterbodies.

(ii) To characterize and compare the trajectories of alluvial margin terrestrialization and their relationship to changes in the river system.

(iii) To determine the geomorphic contributions of each development phase and identify the drivers of terrestrialization.

(iv) To compare geomorphic adjustments with those observed in other similarly developed rivers.

To achieve these objectives, we developed a GIS-based space-for-time substitution approach (Piégay and Schumm, 2003; Fryirs and Brierley, 2012; Dépret et al., 2017), integrating historical hydrosedimentary data and indicators to reconstruct past river trajectories and evaluate the role of anthropogenic pressures in shaping contemporary river dynamics. This approach provides key insights for developing diagnostic frameworks to guide river restoration and support adaptive management strategies.

https://doi.org/10.5194/egusphere-2026-3582
Preprint. Discussion started: 10 July 2026

2.Study area

2.1. Geographical and historical context of the Rhône River watershed

Please use only the styles of this template (MS title, Authors, Affiliations, Correspondence, Normal for your text, and Headings 1–3). The title page must include the title (concise but informative), author first and last names, full institutional addresses of all authors, and correspondence email for proofs. Deceased co-authors should be marked accordingly. After the abstract, the sequence of the sections of your manuscript is introduction, sections of your choice, and conclusions.

The Rhône River, stretching 812 km, originates from the Furka Glacier (2340 m asl) in the Swiss Alps (Canton of Valais). Its watershed spans 98,500 km², with 90,500 km² located in France. The river flows into the Mediterranean Sea, with an average annual discharge of 1700 $m^3 \cdot s^{-1}$, at the Beaucaire gauging station just upstream of the delta (Olivier et al., 2022). The Rhône and its tributaries traverse various geological units (Jura, Massif Central, and Alps) and three major ecoregions: the Alps, the Western Highlands, and the Mediterranean part of the Western Plains, indicating that the Rhône has a complex hydrological regime (glacial, nival, and rainfall regime) (Olivier et al., 2009). Historically, during the Little Ice Age, the Rhône was a multi-thread river with a coarse alluvial load, flowing through unvegetated gravel corridors, often braiding or anabranching.

In the late 19th century, significant channelization (Phase 1) works were undertaken on the river to improve navigation from Lyon to the Mediterranean Sea, including the implementation of dike fields along the terrestrial channel margins. The dike structures exhibit diverse configurations designed to fulfill local correction objectives outlined (Combe and Escudié, 1991; Räpple, 2018). These configurations encompass traditional groin fields (hereafter referred to open fields), various arrangements of lateral dikes, sills, weirs, and distinctive closed dike structures developed by the engineer Henry Girardon. These closed fields consist of a longitudinal submersible dike supported by lateral dikes, forming polygonal structures that extend from the outer margin of the channel to the proximal floodplain margins.

Throughout the latter half of the 20th century, numerous dams were constructed along the river (including 17 diversion schemes; see **Fig. 1**) for hydroelectric power production (Phase 2). As a result of these two engineering phases, the river has largely been transformed into a single-thread channel (Bravard, 2010; Riquier, 2015; Tena et al., 2020). Significant terrestrialization has occurred along the engineered margins, initially triggered by the construction of dike fields and later reinforced by the installation of diversion dams. These developments led to in-dike storage of fine sediments, water level alterations, and changes in the mode of hydrosedimentary connectivity at the floodplain scale (Seignemartin et al., 2023).

https://doi.org/10.5194/egusphere-2026-3582
Preprint. Discussion started: 10 July 2026

125 **Fig. 1: Location of the four studied reaches (channelized and bypassed) along the Rhône River continuum (France). Map created by the authors using watershed and river network data from BD Carthage®**

2.2. Geographical context of the studied reaches

We selected four reaches that have undergone the two major phases of development (channelization and dam construction) and are currently at the heart of the Rhône plan restoration projects **(Fig. 1 and Table 1)**.

https://doi.org/10.5194/egusphere-2026-3582
Preprint. Discussion started: 10 July 2026

i. **Pierre-Bénite (PBN):** Located downstream of Lyon at the confluence of the Saône and Rhône rivers, this reach extends over 12.5 km with an average slope of 0.05%.

ii. **Péage-de-Roussillon (PDR):** Situated approximately 60 km downstream of PBN, this reach has similar characteristics, extending over 14.5 km with a slope of 0.06%.

iii. **Montélimar (MON):** Located 150–200 km downstream of Lyon, this reach is influenced by the upstream confluences of the Isère, Eyrieux, and Drôme rivers, along with western tributaries from the Cévennes region. It spans approximately 14.5 km and has an average slope of 0.08%.

iv. **Donzère-Mondragon (DZM):** Positioned just downstream of MON, this reach includes the confluence with the Ardèche Rivers, occurring approximately two-thirds of the way along its length. It is almost three times as long as the other studied reaches and has a slope of 0.07%.

2.3. Engineering work characteristics of the studied reaches

Channelization works were carried out in all four reaches during the 1880s and 1900s. At PBN, there are 261 dike fields, with the highest density at 20.8 structures per linear kilometer, covering 116 ha. PDR features 234 dike structures, averaging 16.3 structures per kilometer, spanning more than 108.2 ha. MON has 122 dike structures, with an average of 8.4 structures per linear kilometer, lower than that of the other reaches, and covering 93 ha. DZM has 385 dike structures, resulting in an average of 11.6 structures per linear kilometer, and spanning 370.3 ha (**Table 1**).

Dike field areas vary by reach. For closed fields, PDR areas are slightly larger than those of PBN ($p = 0.085$), those of MON are slightly larger than those of PDR, and those of DZM are much larger than those of MON ($p < 6 \times 10^{-8}$), giving the order PBN ≤ PDR ≤ MON < DZM (medians: 0.27, 0.33, 0.46, and 1.35 ha). For open structures, MON areas are smaller than those of PDR ($p = 0.024$), those of DZM are larger than those of MON, while PBN do not differ significantly from those of PDR ($p = 0.53$) or those of DZM ($p = 0.16$), resulting in MON < PDR ≤ DZM ≈ PBN (medians: 0.23, 0.3, 0.4, and 0.43 ha). Width-to-length ratios vary by structure type but show no significant differences across reaches for either closed ($p = 0.31$) or open ($p = 0.27$) dikes.

Diversions occurred at DZM (1952), MON (1957), PBN (1966), and PDR (1977). Average discharges, initially 1035–1480 $m^3 \cdot s^{-1}$, dropped after bypassing to 10–60 $m^3 \cdot s^{-1}$ depending on the site. Following restoration measures, reserved discharges were increased to 75 $m^3 \cdot s^{-1}$ at MON and DZM (2014), approximately 100 $m^3 \cdot s^{-1}$ at PBN (2000), and 50–125 $m^3 \cdot s^{-1}$ at PDR (2014). These values are occasionally surpassed during major floods when the hydroelectric plant's capacity is reached.

Table 1: Characteristics of the four studied reaches (Rhône River, France)

Reach	PBN	PDR	MON	DZM
Reach properties				
Kilometer point (after Lyon city)	KP 3.5	KP 50.5	KP 152.5	KP 170.5
Linear length (lkm)	12.5	14,4	14.5	33
Channel slope (%)	0.05	0.06	0.08	0.07
Mean annual discharge when total (m^3/s)	1030	1050	1494	1500
Channelization features (since 1880-1900s)				
Closed fields (n)	100	89	63	111
Opened fields (n)	122	126	33	236
Other hydraulic structures (n)	39	19	26	38
Total (n)	261	234	122	385
Covered area (ha)	116	108.2	93	370.3
Average density of dike fields (structures/lkm)	20.8	16.3	8.4	11.6
Average cover of the dike fields (ha/lkm)	9.3	7.5	6.4	11.2
Diversion characteristics				
Diversion date	1966	1979	1957	1952
Maximum processed power plant discharge (m^3/s)	1365	1600	1900	1980
Residual flow - before restoration	10-20	10-20	15-60	60
Residual flow - after restoration	100 (since 1999)	50-125 (since 2014)	75 (since 2014)	75 (since 2014)

3. Materials and methods

The first part of this section introduces GIS-based methods for planimetric analysis, designed to characterize the geomorphological evolution of each reach during the last century and model the current submersion frequency of the margins to assess their present hydrological connectivity. The second part focuses on hydrosedimentary change indicators, providing insights into the contribution of various development phases and the underlying drivers and processes.

3.1. Geomorphic adjustments analyzed using GIS

3.1.1. Planform dataset and general GIS processing

We assessed fluvial planimetric changes using georeferenced aerial photographic archives within a GIS, following established methodologies (e.g., Bryant and Gilvear, 1999; Winterbottom, 2000; Gilvear and Bryant, 2003). Previous GIS studies of the Rhône River mainly examined side channels and floodplains (Riquier et al., 2015, 2017; Dépret et al., 2017; Tena et al., 2020; Arnaud et al., 2021); this study extends the analysis to margin terrestrialization.

Planform features were extracted using GIS software (ArcMap™ 10.8) through georeferencing and vectorization of aerial images from the National Institute of Geographical and Forest Information (IGN) database. For each reach, we selected specific series to assess the impact of each developmental phase on the evolution of the active channel and margin terrestrialization processes. These series provided insights into the post-channelization/pre-diversion changes during the early to mid-20th century, rapid transformations following diversion, and long-term adjustments leading to the current conditions.

The aerial photographs, captured between the 1930s and 2000s, had a 1-m resolution, whereas orthophotographs from the 2000s, with a 50-cm pixel resolution, served as the georeferencing base. Comprehensive details of the photographs, including resolution, acquisition technique, color gradient, and associated river discharge, are provided in **Appendix A, Table 1**. To establish a reference point predating the river engineering works, we also utilized a topographical map dating from 1857 to 1876, at a 1/10,000 scale, commonly referred to as the "1860 Atlas." To improve fit at the dike field scale, photographs were georeferenced by subdividing reaches into 2 km polygons, reducing spatial distortions from differing image coverages (Seignemartin et al., 2023). Within each subpart, 10–20 evenly distributed ground control points—based on dike crossings, bridges, and buildings—were used. RMSE values ranged from 5.3 ± 1.3 m (1947 in PBN) to 1.8 ± 1.1 m (2001 in MON), indicating good rectification quality (**Appendix A, Table 2**; Gurnell, 1997; Arnaud et al., 2015). We digitized the boundaries between water and land for each photograph series, at a spatial resolution of 1:500–1:1500, adjusted for image quality. Canopy cover often obscured the boundaries, so we interpreted them 2–6 m from the vegetation edge, using visible breaks in the tree cover to locate the riverbed (Liébault and Piégay, 2002; Depret et al., 2017; Tena et al., 2020). For each date, this produced polygons of terrestrial versus aquatic areas, which we then analyzed using basic spatial operations (erasure, intersection) to quantify planimetric land-use changes within the areas of interest.

3.1.2. Margin dedicated GIS processing

To delineate the extent of terrestrialization, we used a vector layer corresponding to the spatial extent of the dike fields (Räpple, 2018) which we updated and completed. For this purpose, we used historical maps (bathymetric map from the Compagnie Nationale du Rhône from 1897, Branciard cartographic map from 1910), in combination with the aerial photographs (**Appendix A, Table 1**). We acquired diachronic patterns of terrestrialization in the dike fields by overlaying the multi-date series of polygons onto this dataset after removing the subsequently eroded areas. We conducted a statistical analysis on a dataset consisting of 763 dike fields. These dike fields were distributed as follows: 178 at PBN, 215 at PDR, 98 at MON, and 272 at DZM (see **Table 2** for details). Due to their specificity, certain dike configurations such as half-open structures similar to those of wing groins as described by Przedwojski (1995), were excluded from the planimetric analysis. Additionally, dike fields that were not directly adjacent to the main channel and those displaying clear signs of human modifications, such as maintenance or engineering work, were also excluded.

https://doi.org/10.5194/egusphere-2026-3582
Preprint. Discussion started: 10 July 2026

Table 1: Dike fields studied on the four reaches

	PBN	PDR	MON	DZM
Open fields	112	96	67	170
Closed fields	66	119	31	102
Total studied dike fields	178	215	98	272
Excluded dike fields	6	18	10	45

3.2. Characterization of planform changes

3.2.1. Main channel and side channel water surface loss

In the literature, the active channel includes low-flow channels and unvegetated bars (Liébault and Piégay, 2002; Haschenburger and Cowie, 2009). For hydromorphological analyses, we distinguish the main channel from side channels, which we collectively refer to as waterbodies. Engineered margins represent the full extent of the dike fields, whether closed or open.

Main and side channel evolutions were studied following the same approach. To assess the evolution of these two waterbody types throughout the 20th century, we calculated their surface area for each map and photo series listed in **Appendix A, Table 2**. Different metrics capturing the same phenomenon are provided, allowing for comparisons between sites and among river systems.

The rate of waterbody surface loss was calculated with the following durations for the retraction process: for Phase 1 (from 1860, the historical reference before channelization works) – PBN: 94 years, PDR: 114 years, MON: 86 years, DZM: 87 years; and for Phase 2 (from dam works to the reference date) – PBN: 54 years, PDR: 35 years, MON: 61 years, DZM: 62 years. For example, the absolute rate of waterbody area loss ($ha \cdot y^{-1}$) is calculated according to Eq (1).

$$TA \cdot y^{-1} = \frac{\sum(\text{retracted waterbody area})_t - (\text{retracted waterbody area})_{t-1}}{(t-(t-1))} \quad (1)$$

The relative rate of waterbody surface loss (reach-relative percentage per year; $ha \cdot y^{-1}$) allows for the removal of the size effect (i.e., the linear length of the reach) and facilitates comparison between reaches. Another metric that allows for the removal of the reach-size effect is the average width, calculated by dividing the total surface area by the channel's linear length, providing a standardized measure of width reduction.

3.2.2. Quantitative and qualitative assessment of terrestrialization

Quantifying margin terrestrialization

We examined the progression of terrestrialization by considering the terrestrial area percentages (TA%, %) within each dike field using Eq. (2).

$$TA\% = (\text{mineral or vegetated surface within the dike field / total area of the dike field}) \times 100 \quad (2)$$

The cumulated terrestrialized areas (ha) were calculated by summing the terrestrialized areas within all the dike fields across the entire reach for the date corresponding to the photo series, according to Eq. (3).

$$TA = \sum \text{mineral or vegetated surface within each dike field at a specified date} \quad (3)$$

Terrestrialization rates were calculated over two phases: Phase 1 (dike works to pre-dam reference) – PBN: 76 years, PDR: 89 years, MON: 67 years, DZM: 61 years; Phase 2 (dam works to reference) – PBN: 42 years, PDR: 29 years, MON: 51 years, DZM: 57 years. For example, the absolute rate of terrestrialization ($ha \cdot y^{-1}$) is calculated according to Eq. (4).

$$TA \cdot y^{-1} = \frac{\sum(\text{terrestrialized area})_t - (\text{terrestrialized area})_{t-1}}{(t-(t-1))} \quad (4)$$

The relative rate of terrestrialization (reach-relative percentage per year; $ha \cdot y^{-1}$) allows for the removal of the size effect (i.e., the linear length of the reach). Terrestrialization intensity reflects the rate of in-dike terrestrialization per unit river length ($m^2 \cdot km^{-1} \cdot y^{-1}$)

Terrestrialization patterns

Inspired by Sukhodolov et al. (2002) inter-groin deposition patterns, the qualitative analysis of chronoplanimetry is based on the terrestrialization pattern classification detailed in Seignemartin *et al.* (2023). Based on the prevalence of specific forms, terrestrialization timeframes, and structural characteristics, the classification includes five main types:

i. **Aquatic**: The dike structure is predominantly aquatic, with aquatic surface covering more than 85% of the dike's extent.
ii. **Lateral**: The dike structure exhibits partial terrestrialization, primarily along its lateral edges, adjacent to the riverbank.
iii. **Concentric**: The dike structure is highly terrestrialized, although areas with progressive concentric closures may still retain aquatic areas.
iv. **After-Dam Uniform**: The dike structure's surface represents a uniformly terrestrialized area resulting from the lowering of water levels following diversion or dam construction.
v. **Complex**: The dike structure's surface exhibits varying degrees of terrestrialization. Stationary factors such as the presence of former side channels, old islands, and original dike configurations contribute to complex and diverse forms.

Note that some rare dike fields were filled during the early 20th century, and the lack of chrono-planimetric data prevents us from linking them to a specific pattern.

3.2.3. Remaining overflow-driven lateral connectivity of engineered margins

The hydrological connectivity of alluvial margins was estimated using an overflow-driven lateral submersion model, originally developed by Dzubakova *et al.* (2015). This model integrates a LiDAR-derived DEM (2010), rating curves, and daily discharge series spanning 1986–2010.

Elevation data were obtained from an airborne LiDAR DEM collected by IGN in 2010, with a 2 m spatial resolution and 0.2 m vertical accuracy. Pulse density ranged from 1 to 2 pulses per m², each covering roughly 0.4 m in diameter. Average

https://doi.org/10.5194/egusphere-2026-3582
Preprint. Discussion started: 10 July 2026

elevations for each dike field were calculated over the full extent of their delineated shapes, allowing assessment of their vertical position relative to water levels.

Rating curves converted discharge values into water levels, which were then projected across the floodplain. Water levels were assumed uniform within each cross-section, with a gradual decline downstream. This produced a raster-based representation of lateral connectivity, where each pixel indicates attributes such as submersion frequency ($d \cdot y^{-1}$).

Finally, the relationship between average dike field submersion frequency—used as a proxy for hydrological connectivity—and terrestrialization rate was analyzed using a generalized linear model (GLM) with a binomial link function, since the data are proportions bounded between 0 and 1. The glm function in R (v4.0.3) was applied, and the proportion of deviance explained (D^2) was calculated using the Dsquared function from the modEvA_package version 3.45 (https://CRAN.R-project.org/package=modEvA).

3.3. Hydrosedimentary indicators of terrestrialization

3.3.1. Processes and drivers of terrestrialization

Our prior research highlighted two key processes contributing to terrestrialization (Seignemartin et al., 2023). The first process that can result in sediment deposition is fine sediment accumulation (PROCESS 1). This process is initiated by the installation of dike fields, which create areas with reduced shear stress (DRIVER 1). The second process leading to the emergence of terrestrial surfaces involves a decrease in water levels (PROCESS 2), which can occur through either riverbed incision caused by the channelization—which increases shear stress within the channel (DRIVER 2)—or a reduction in water discharge due to diversion, resulting in lower water levels (DRIVER 3). Finally, we also considered gravel extraction (DRIVER 4), which reduces alluvial stocks and can create erosion pits, thereby contributing to riverbed incision (**Table 3**).

Table 2: Processes and drivers of terrestrialization

PROCESS 1: Fine sediment accumulation	PROCESS 2: decrease in water levels leading to terrestrial emergence		
DRIVER 1: dike fields creating areas with reduced shear stress	DRIVER 2: riverbed incision caused by the channelization	DRIVER 3: reduction in water discharge due to diversion	DRIVER 4: riverbed incision caused by gravel extraction

Riverbed and water level evolution

Riverbed and water level changes (referred to as "free surface elevation") were assessed using riverbed elevation data from Parrot (2015) for three periods (**Table 4**): (i) the baseline in 1897, (ii) after channelization and the recent bypass in 1982, and

(iii) the current state following channelization and diversion in 2008. Bathymetric transects were collected at 500-m intervals (Topographic Data Base of the Rhône; IGN, 2010).

Water levels were represented using low-flow measurements from 1902 to characterize conditions shortly after early channelization. Pre-diversion water levels were taken from a 1945 low-water survey at 560 $m^3 \cdot s^{-1}$. Post-diversion conditions were based on 2010 data from the BDT Rhône, reflecting minimum flow conditions in the bypassed reach.

Table 3: Datasets associated with the riverbed and water level evolution on the four reaches during the 20th century

Date	Source	Development state	Survey step or accuracy (m)	Discharge indications	Informed state	Comparisons and insights
Riverbed elevation						
1897 (PBN-PDR-MON) 1907 (DZM)	Compagnie Nationale du Rhône (Processed by Parrot, 2015)	Channelization in prep. or begun (1897)	500 m	Total discharge	Reference state at the end of the 19th century	Potential effect on incision tendencies due to: Channelization (↗?) & gravel extraction (↗?).
1968 (PBN) 1969-74 (PDR) 1957-62 (MON) 1953-57 (DZM)		~50-70 years after channelization, A few years after flow diversion except for PDR (before)	500 m	Total discharge	Post-channelization – recently bypassed (1982)	
2006-2009	Topographic Data Base of the Rhône (Processed by Parrot, 2015)	More than 100 years after channelization, 40 to 60 years after flow diversion	500 m	Residual discharge	Current “post-channelization – post-diversion” (2008)	Situation with both developments. Potential effect on incision tendencies of the: residual discharge (↘?) & gravel extractions (↗?).
Water levels						
1902	*Fascicule Armand des pentes du Rhône*	Just after channelization	Step: 1000 m	Low water	Reference state at the beginning of the 20th century	Channelization effect on the water level NB: similar discharge conditions
1945	Compagnie Nationale du Rhône	60 years after channelization, before flow diversion	Step: 1000 m	Low water (560 m^3/s)	Reference state at the end of phase 1	
2010	Topographic Data Base of the Rhône	More than 100 years after channelization, 40 to 60 years after flow diversion	Accuracy: 20 cm	Residual discharge (20 m^3/s)	State in average conditions at the end of phase 2	Flow diversion impact on the water level in a channelized situation (cumulative impact) NB: comparing a rare low water condition before diversion and a residual - and so “average” - condition after diversion necessarily underestimate the real impact/ gap compared to both average conditions.

https://doi.org/10.5194/egusphere-2026-3582
Preprint. Discussion started: 10 July 2026

Data on gravel extraction and tributary bedload

The data on gravel extraction volumes include extraction records spanning from 1954 to 2010 (Acthys, 2017). Typically, extractions are documented (KP, date, and volumes) from the commencement of dam construction work. Prior to this phase, no consistent records of gravel extractions exist, making it impossible to account for them when assessing their potential impact on riverbed elevation during Phase 1. The data on alluvial inputs from tributaries come from the work of the Rhône Sediment Management Master Plan (Laval and Fantino, 2020).

4. Results

4.1. Planform monitoring of the riverscape features throughout the development phase

4.1.1. Main channel narrowing

Across the four reaches, the main channel experienced substantial narrowing over the 20th century, with varying contributions from channelization (Phase 1) and diversion (Phase 2) depending on the reach (**Fig. 2**).

https://doi.org/10.5194/egusphere-2026-3582
Preprint. Discussion started: 10 July 2026

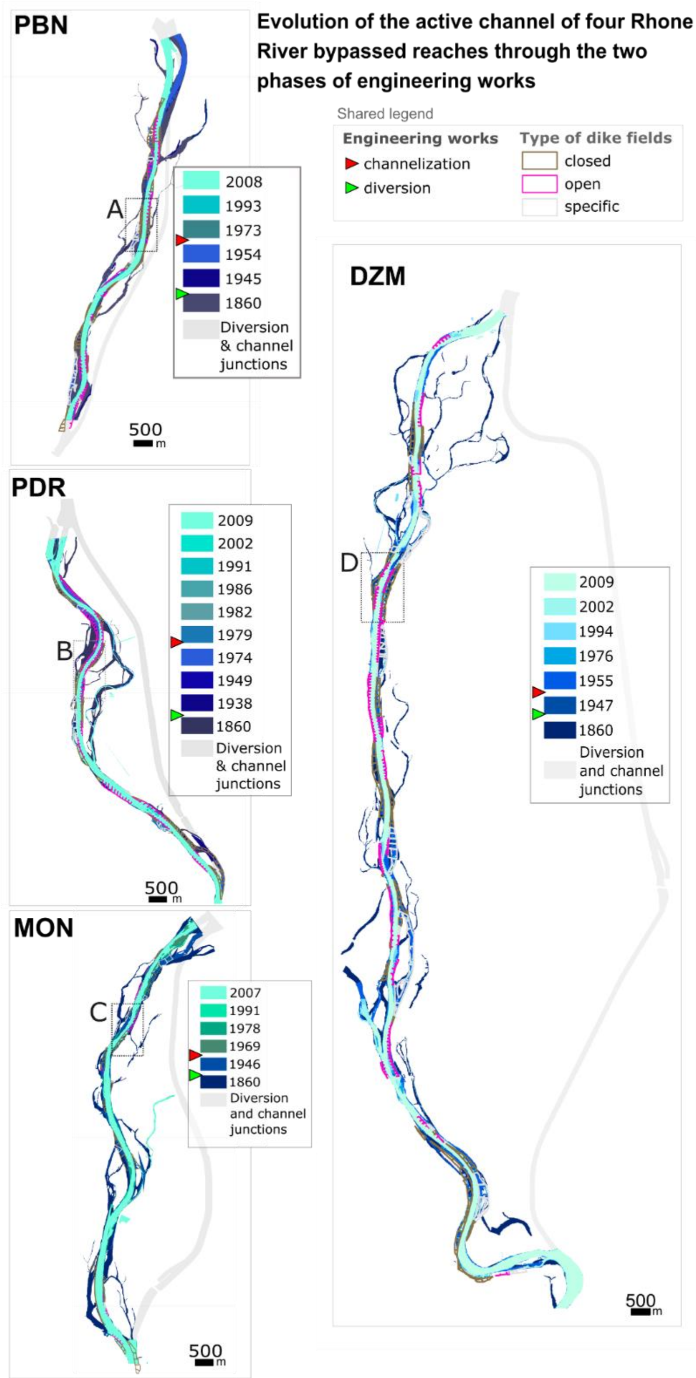

Fig 2: Rhône channel planform evolution in the four studied reaches (PBN, PDR, MON, DZM) according to two main contemporary engineering phases. The dashed gray frames (A, B, C, D) refer to the areas depicted in Fig 4.

https://doi.org/10.5194/egusphere-2026-3582
Preprint. Discussion started: 10 July 2026

During Phase 1, aquatic areas decreased by −31.2% at PBN, −28% at PDR, −10.4% at MON, and −13.4% at DZM (**Table 5A**). This corresponds to a reduction in average channel width, from 275 to 189 m at PBN, 271 to 195 m at PDR, 277 to 248 m at MON, and 255 to 221 m at DZM.

In Phase 2, the reductions continued: −16.2% at PBN, −16.5% at PDR, −29.9% at MON, and −24.1% at DZM. Channel width further narrowed, from 189 to 145 m at PBN, 195 to 151 m at PDR, 248 to 165 m at MON, and 221 to 159 m at DZM (**Table 5A**).

Across the four reaches, Phase 1 and Phase 2 contributed to main channel narrowing in the following ratios: PBN (2:1), PDR (2:1), MON (1:3), and DZM (1:2). ratios emphasize the contrasting roles of the two phases, with Phase 1 driving most of the losses at PBN and PDR, while Phase 2 had the stronger effect at MON and DZM.

https://doi.org/10.5194/egusphere-2026-3582
Preprint. Discussion started: 10 July 2026

Table 5: Diachronic analysis of (A) main channel retraction and (B) side channels, (C) dike field terrestrialization, and river bed elevation across four sectors (PBN, PDR, MON, DZM) during two engineering phases. Base = state before engineering sequences (1860 for A and B; 1890 for C; 1890s-1900s for D), P1 = Phase 1 (channelization sequence), P2 = Phase 2 (Diversion dam sequence), Total: cumulated sequences.

Reach	PBN				PDR				MON				DZM			
Length (kml)	11.2				11.1				14.1				32.6			
Reference sequence/date	BASE	P1	P2	TOTAL	BASE	P1	P2	TOTAL	BASE	P1	P2	TOTAL	BASE	P1	P2	TOTAL
A- MAIN CHANNEL																
Area - Active channel (ha)	307.8	211.7	162	x	300.2	216.3	167.6	x	389	348	232.5	x	831.9	720.5	542.6	x
Median width (m)	275	189	145	x	270	195	151	x	276	247	165	x	255	221	166	x
Rate of width retraction (m. y-1)	x	0.91	0.81	0.88	x	0.66	1.26	0.8	x	0.34	1.34	0.76	x	0.39	0.89	0.60
Percentage of retraction (%1860)	x	-31.2	-16.2	-47.4	x	-28	-16.2	-44.2		-10.4	-29.9	-40.2	x	-13.4	-21.4	-34.8
Phase contribution in retraction (%)	x	65.9	34.1	x	x	63.3	36.7	x	x	26.2	73.8	x	x	38.5	61.5	x
Absolute rate of area loss (ha. y-1)	x	-1.02	-0.92	-0.99	x	-0.74	-1.4	-0.89	x	-0.48	-1.9	-1.06	x	-1.28	-2.87	-1.94
Relative rate of area loss (%. y-1)	x	-0.33	-0.3	-0.32	x	-0.25	-0.46	-0.3	x	-0.12	-0.49	-0.27	x	-0.15	-0.35	-0.23
Associated duration based on diachronic series (y)	x	94	54	148	x	114	35	149		86	61	147	x	87	62	149
B - SIDE CHANNELS																
Area - Side channels (ha)	79.7	10.8	3.5	x	98.6	14	23.1	x	81.6	10.3	10.1	x	76.2	31.4	8.1	x
Median cumulated width of side channels (m)	71	10	3	x	89	13	21	x	58	7	7	0	23	10	2	
Rate of width retraction (m. y-1)	x	0.65	0.13	0.46	x	0.67	-0.23	0.46	x	0.59	0	0.35	x	0.15	0.13	0.14
Percentage of retraction (%1860)	x	-86.4	-9.2	-95.6	x	-85.8	9.3	-76.5		-87.3	-0.2	-87.6	x	-58.8	-30.6	-89.4
Phase contribution in retraction (%)	x	90.4	9.6	x	x	112	-12	x	x	99.7	0.3	x	x	65.8	34.2	x
Absolute rate of area loss (ha. y-1)	x	0.73	0.14	0.51		0.74	-0.26	0.51	x	0.83	0	0.49	x	0.51	0.38	0.46
Relative rate of area loss (%. y-1)	x	-0.92	-0.17	-0.65	x	-0.75	0.27	-0.51	x	-1.02	0	-0.6	x	-0.68	-0.49	-0.6
Associated duration based on diachronic series (y)	x	94	54	148	x	114	35	149		86	61	147	x	87	62	149
C- DIKE FIELDS																
Cumulated extent of studied dike fields (ha)	86.3				77.2				65.4				317.25			
Cumulated terrestrialized area (ha)	0	38	35.2	73.2	0	27.6	31.3	58.9	0	17.5	43.1	60.6	0	104.9	176.5	281.4
Percentage of terrestrialization (%)	x	44	40.8	84.8	x	35.7	40.6	76.3	x	26.8	65.9	92.7	x	33.1	55.6	88.7
Phase contribution in terrestrialization (%)	x	52	48	x	x	47	53	100	x	29	71	x	x	37	63	x
Terrestrialization intensity ($m^2.kml^{-1}. y^{-1}$)	x	528.2	591.5	557.2	x	296	808.4	446.7	x	209.8	841.7	539.3	x	354.8	1066.5	725.6
Absolute rate of terrestrialization ($ha. y^{-1}$)	x	0.59	0.65	0.62	x	0.3	0.89	0,49	x	0.31	0.7	0.52	x	0.31	0.71	0.52
Relative rate of terrestrialization ($\%. y^{-1}$)	x	0.69	0.76	0.72	x	0.42	1.16	0.64	x	0.48	1.08	0.79	x	0.58	0.9	0.75
Associated duration based on engineering setting and diachronic series (y)	x	64	54	118	x	84	35	119	x	56	61	117	x	57	62	119
D - RIVER BED ELEVATION																
Incision (m)	x	-2.11	-1.94	-4.05	x	-0.27	-0.8	-1.07	x	-1.28	-0.01	-1.29	x	0.08	-0.72	-0.64
Magnitude of Incision (cm.y-1)	x	-3	-5	-3.7	x	-0.4	-2.1	-1	x	-2.1	0	-1.2	x	0.2	-1.3	0.6
Associated duration based on historical surveys (y)	x	71	39	110	x	72	38	110	x	60	50	110	x	46	54	110

https://doi.org/10.5194/egusphere-2026-3582
Preprint. Discussion started: 10 July 2026

The point sizes in **Figure 3** indicates the water discharge recorded during each aerial photography campaign, allowing trends to be interpreted considering water discharge variations. The particularly low discharge in the 1949 PDR series (342 m³/s) explains the unusually small channel surface observed at that date. This accentuates the decline already evident since 1938, while the subsequent recovery (1948–1974) did not reverse the overall downward trend (Area1974 < Area1938; **Fig. 3**). Moreover, side channels appear to be relatively unaffected by changes in water discharge, significant fluctuations in water discharge do appear to have an impact on the main channel surface. The MON 1978 series, with a total discharge of 2210 $m^3 \cdot s^{-1}$ exceeding the maximum processing capacity of the power plant (1900 $m^3 \cdot s^{-1}$), suggests an overflow of residual discharge into the bypassed reach. A similar situation occurred at DZM in the 1994 series ($Q_{total} = 2220\ m^3 \cdot s^{-1}$) and was also likely in the 1955 series, despite the lower discharge of 1110 $m^3 \cdot s^{-1}$. These anomalies may be explained by temporary malfunctions of hydroelectric facilities, which can reduce the volume of processed water and consequently increase the discharge released into the bypassed section.

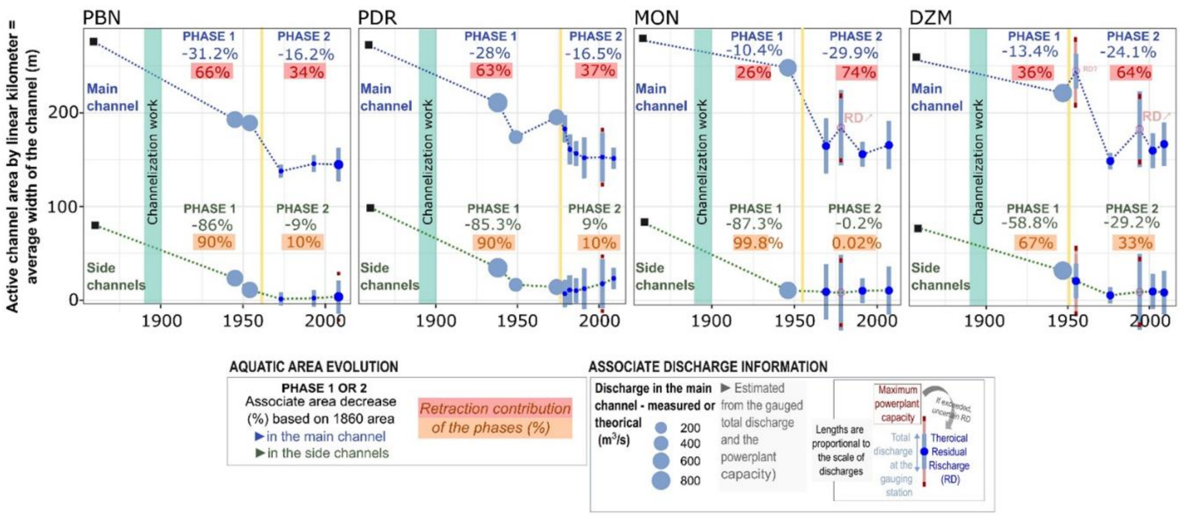

Fig. 3: Active and side channel retraction according to the engineering phases

Side channel areas and features underwent a significant loss between 1860 and the early 20th century. The implementation of corrective measures—primarily involving the closure or disconnection of these channels from the main course—led to the disappearance or substantial reduction of many side channels, resulting in the loss of aquatic areas and disappearance of numerous islands. Only a few remnants, mainly isolated features such as oxbow lakes, now bear witness to the former river morphology. This transformation is clearly illustrated in **Figure 2** by the shift from widespread dark blue areas to a limited number of lighter-shaded features. Historically, these side channels played a crucial role in shaping the floodplain, creating islands and a mosaic of alluvial habitats. Depending on the reach, Phase 1 alone accounted for between 67% and 99.8% of the total reduction in side channel area (**Fig. 3**).

From an inter-reach perspective, Phase 1 resulted in substantial losses of side channel water areas: −86.4% (−77.2 ha) in PBN, −85.3% (−93.8 ha) in PDR, −87.2% (−100.2 ha) in MON, and −58.8% (−146.0 ha) in DZM, relative to those in the 1860 baseline (**Table 5B**). Phase 2 continued this pattern of decline, although with more moderate additional surface losses: −9% (−8.2 ha) in PBN, −0.2% (−0.3 ha) in MON, and −29.2% (−72.6 ha) in DZM. The gain in aquatic area observed during Phase 2 in PDR (+9.3%, i.e., +9.1 ha) likely reflects the impact of restoration efforts, the presence of the Platière Nature Reserve, and associated ecological management measures.

4.1.2. Engineered margins undergoing terrestrialization

A two phases trajectory of terrestrialization

Currently, 87% (474 ha) of the engineered margins are terrestrial, whereas only 13% of their surface remains aquatic. Dike fields exhibit chrono-planimetric patterns that are divided into five classes, found across all four reaches (**Fig. 4B**). They are distributed as follows: 49% are lateral, 23% are complex, 9% are concentric, 9% are after-dam uniform, and 6% are aquatic patterns. A few (3%) were already terrestrialized before the first photograph series.

Dike fields exhibit chrono-planimetric patterns, with terrestrialization unfolding in two distinct phases that reflect the historical trajectory of engineering development. Within each reach, the impacts of both phases can be distinguished. In the mid-20th century, prior to the diversion of the reaches, 34% (187 ha) of intra-structure surfaces (across all reaches; i.e., in 799 dike fields covering 546 ha) had become terrestrial. After a sufficiently rapid post-diversion adjustment at the end of the 2000s (**Fig. 4A**), 87% (474 ha) of intra-structure surfaces are now being terrestrial. The older deposit areas, represented by blue and green surfaces, are primarily located at the rear of the dike fields, often arranged laterally with a simple shape (**Fig. 4B**). Post-diversion areas, indicated by warm colors, complete the polygonal shapes, entirely or partially filling the extent of the dike structure.

https://doi.org/10.5194/egusphere-2026-3582
Preprint. Discussion started: 10 July 2026

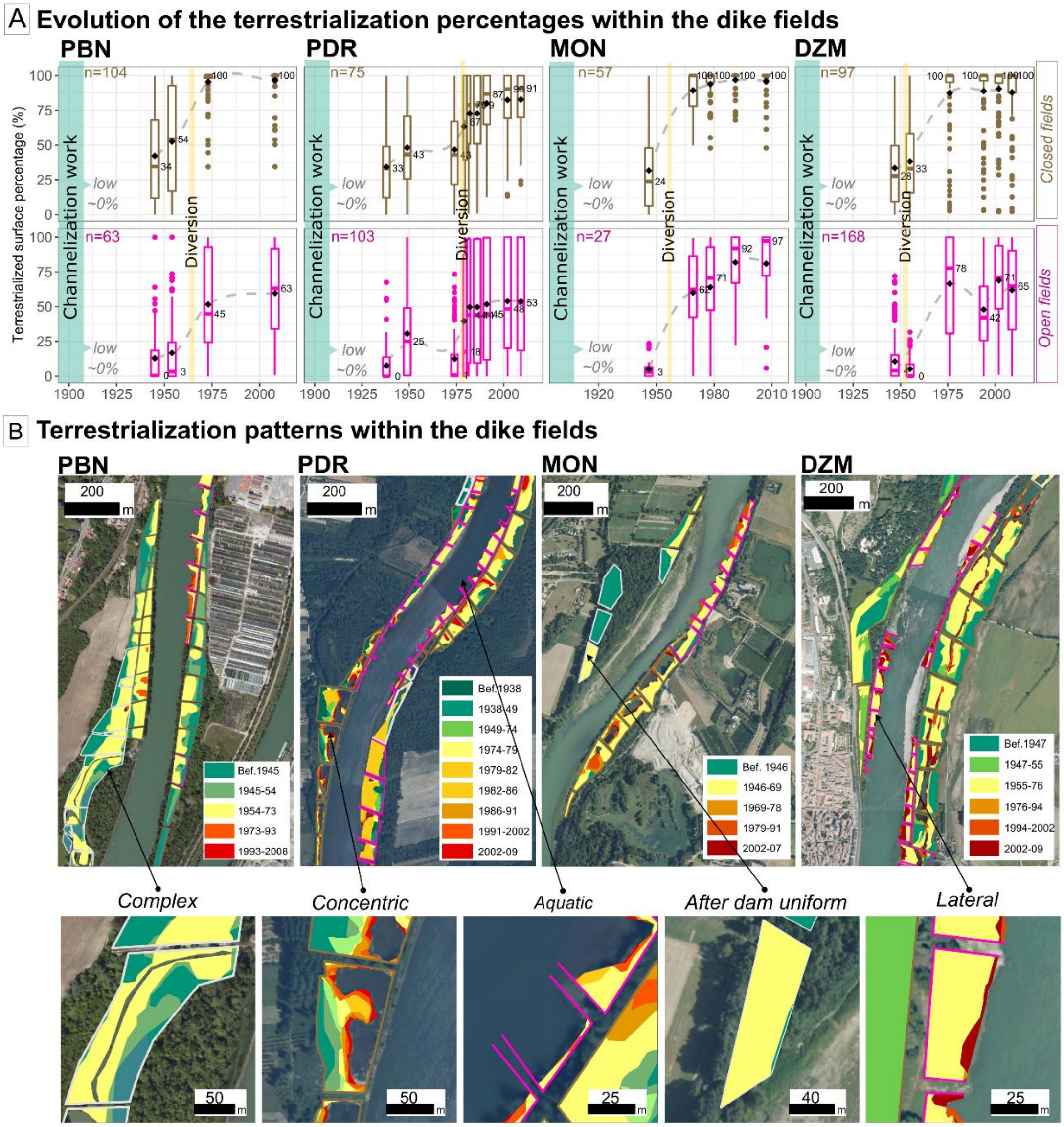

Fig. 4: Terrestrialization within the dike fields. (A) Evolution of the terrestrialization percentages within the dike fields; (B) Terrestrialization patterns within the dike fields. Maps created by the authors using IGN orthophotographs from the 2000s (see Appendix A1 for data sources).

The influence of dike field type on terrestrialization patterns across phases

Closed fields began their terrestrialization process from their installation in the early 20th century, with 40.8% (99 ha) of the total closed field area (334 closed fields covering 243 ha) already being terrestrial before the diversion. In contrast, open fields predominantly remained aquatic before the diversion, with only 17% (22 ha) of the total open field area (360 open fields covering 243 ha) having transitioned to terrestrial environments. Following the diversion, a substantial increase was observed in terrestrialized areas in all reaches. In most cases, the closed fields underwent nearly complete transition, with 91% of terrestrial area (cumulated 223 ha). Open fields also displayed an increasing trend toward terrestrialization over the 20th century, reaching 68% terrestrial area (cumulated 128 ha). In terms of chronoplanimetry, closed fields (n = 335) exhibit high heterogeneity of terrestrialization patterns (**Fig. 4B**), with 37% being lateral, 25% complex, 20% concentric, 12% after-dam uniform, and less than 1% remaining aquatic. For open fields (n = 362), more than 70% are lateral patterns, nearly 12% are still aquatic, and 8% are after-dam uniform patterns. However, open fields show significantly fewer complex patterns (8%). In the case of specific dike fields (n = 102), their terrestrialization rates closely match those of closed fields (39% at the end of Phase 1 and 93% at the end of Phase 2). Considering their distinctive geometry and placement (side channel, closure for island), the "complex" type is predictably prevalent, constituting 72%.

Terrestrialization patterns across phases and dike field types: reach-specific responses

Across all dike-field types, terrestrialization in Phase 1 reached 44% at PBN (38 ha), 36% at PDR (27.6 ha), 27% at MON (17.5 ha), and 33% at DZM (104.9 ha). In Phase 2, these values rose to 41% at PBN (35.2 ha), 41% at PDR (31.3 ha), 66% at MON (43.1 ha), and 56% at DZM (176.5 ha). Combined, total terrestrialization reached 85% at PBN (73.2 ha), 76% at PDR (58.9 ha), 93% at MON (60.6 ha), and 89% at DZM (281.4 ha). Phase contributions differed among sites: at PBN, 52% of terrestrialized area originated from Phase 1; at PDR, 47%; at MON, 29%; and at DZM, 37% (Table 5C).

The intensity of terrestrialization enables comparison of terrestrialized surfaces normalized to reach length and phase duration. In Phase 1, the intensity of terrestrialization was highest in PBN, at 528.2 $m^2 \cdot km^{-1} \cdot y^{-1}$, followed by DZM (354.8 $m^2 \cdot km^{-1} \cdot y^{-1}$), PDR (296 $m^2 \cdot km^{-1} \cdot y^{-1}$), and MON (209.8 $m^2 \cdot km^{-1} \cdot y^{-1}$). In Phase 2, the intensity of terrestrialization was highest in DZM, at 1066.5 $m^2 \cdot km^{-1} \cdot y^{-1}$, followed by MON (841.7 $m^2 \cdot km^{-1} \cdot y^{-1}$), PDR (808.4 $m^2 \cdot km^{-1} \cdot y^{-1}$), and PBN (591.5 $m^2 \cdot km^{-1} \cdot y^{-1}$).

As a result, site ranking differs between the two metrics. In Phase 1, DZM showed a moderate percentage (33%) but a relatively high intensity (354.8 $m^2 \cdot km^{-1} \cdot y^{-1}$), placing it ahead of PDR in intensity even with a lower proportion of terrestrialized area. In Phase 2, MON reached the highest percentage (66%), yet DZM displayed the strongest intensity (1066.5 $m^2 \cdot km^{-1} \cdot y^{-1}$). Similarly, PBN and PDR had identical percentages in Phase 2 (41%) but PDR exhibited a much higher intensity. These differences highlight that percentages and intensity values capture distinct aspects of terrestrialization dynamics.

In closed fields during Phase 1, the percentage of terrestrialized surfaces varies significantly across reaches (Kruskal–Wallis *p*-value ≤ 0.001), with "before diversion" terrestrialized surfaces ranking as PBN > PDR > DZM > MON (median: 54%, 43%, 28%, and 24%; corresponding interquartile ranges [IQRs]: 76, 45, 40, and 41). The associated IQRs are substantial, highlighting the diverse terrestrialization situations within each reach, notably with substantial variability at PBN. In open fields, the percentage of pre-bypass terrestrialized surface is not significantly different across reaches (Kruskal–Wallis *p*-value = 0.57), with "before diversion" terrestrialized surfaces showing similar values: PBN ≈ PDR ≈ MON ≈ DZM (median: 3%, 1%, 3%, and 4%; corresponding IQRs: 24, 16, 7, and 15).

In Phase 2, the percentage of terrestrialized surfaces in closed fields is very high in every reach (Fig. 4A) but differed among reaches (Kruskal–Wallis, $p \leq 0.001$), with terrestrialized surfaces ranking PBN ≈ MON ≈ DZM > PDR (medians: 100%, 100%, 91%, and 100%, respectively; IQRs: 0, 0.4, 13, and 30, respectively). However, in open fields, the percentage of terrestrialized

https://doi.org/10.5194/egusphere-2026-3582
Preprint. Discussion started: 10 July 2026

surface in Phase 2 also varies significantly across reaches (Kruskal–Wallis *p*-value ≤ 0.001), with terrestrialized surfaces ranking as MON > DZM ≈ PBN > PDR (median: 98%, 65%, 63%, and 53%; corresponding IQRs: 28, 57, 58, and 81). The associated IQRs underscore the diverse terrestrialization situations within the reaches themselves, particularly with substantial variability at PDR. Additionally, it is noteworthy that the IQRs of the terrestrialization percentage distributions are larger in Phase 1 than in Phase 2 in closed fields across all reaches, whereas they are larger in Phase 2 in open fields. At MON, the Phase 2 IQRs are lower (6.5–45.5, maximum in 1978, in open fields; 0–22, maximum in 1969, in open fields). When paired with higher terrestrialization averages, these values indicate a more consistent overall shift toward terrestrialization in open fields.

The five types of chrono-planimetric patterns are represented across every reach (**Fig. 4B**). Concentric patterns are particularly abundant in closed fields at PDR (n = 32 on 75) and DZM (n = 17 on 99), whereas aquatic patterns predominate in open fields at PDR (n = 24 on 103). Complex patterns are notably prevalent in closed dike fields (n = 42 on 99), and specific patterns occur frequently in the braided and anastomosed forms of DZM (n = 37 on 44).

4.1.3. Link between channel narrowing and dike field terrestrialization rates

The terrestrialization rate of the dike fields is significantly correlated ($R^2 = 0.8$, $p = 0.003$) with the channel narrowing rate during the development phases (see **Fig. 5** and data from **Table 5**). This linear relationship is not observed at the level of the side channels. As margins, the dike fields terrestrialized proportionally but more strongly (rate x2) with channel narrowing. Phase 1 and Phase 2 exhibit differences in narrowing and terrestrialization rates, with Phase 1 showing a lower rate than in Phase 2, likely due to the underlying drivers at work (sedimentation or lowering of water levels) and the system's capacity to adjust to these alterations. These rates tend to obscure the temporal dynamics of adjustment, such as post-dam dynamics in which an initial, marked response is typically followed by a phase of asymptotic relaxation. However, in terms of general trends, the PBN reach was significantly impacted during Phase 1 and underwent a Phase 2 of comparable magnitude, whereas the other reaches, though less affected in Phase 1, exhibit much higher rates in Phase 2. Therefore, understanding the underlying drivers is essential to explain these inter-reach variations.

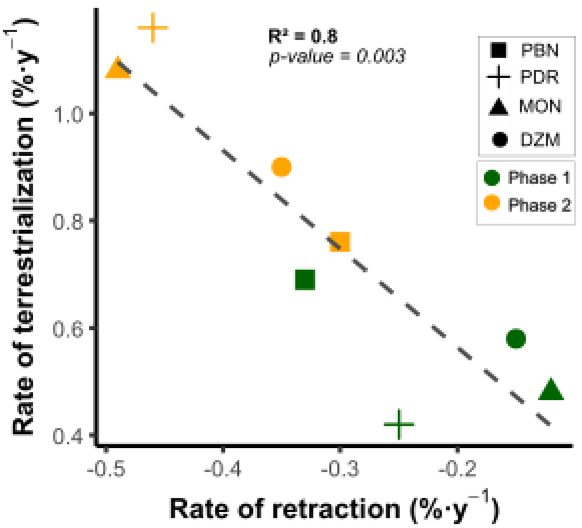

Fig. 5: Correlation between terrestrialization rate in dike fields and main channel retraction rate (data from Table 5)

4.2. Investigating terrestrialization drivers using key hydrosedimentary indicators

4.2.1. Impact of the development phases on riverbed elevation

The elevation surveys of the riverbed show that all reaches experienced incision during the 20th century: on average, around 1 m for PDR, MON, and DZM, and four times as much at PBN (averaging −4.05 m).

However, engineering phases displayed heterogeneous patterns of riverbed incision across reaches. As shown in **Table 5D**, PBN and MON exhibit significant incisions in Phase 1, averaging −2.11 and −1.28 m, respectively. Surprisingly, PDR and DZM show low incision or even a slight aggradation (at −0.27 and +0.08 m, respectively) but substantial incisions in Phase 2, reaching −0.8 m for PDR and −0.72 m for DZM. PBN displays an even greater magnitude in Phase 2 (−4.6 cm·y^{-1}) than in Phase 1 (−2.8 cm·y^{-1}), whereas the MON riverbed remains stable.

The evolution of riverbed elevation exhibits pronounced variations within each reach (see **Fig. 6A and B**). At PBN, the entire linear section undergoes riverbed incision during both Phase 1 and Phase 2, with only minor exceptions: a small area near KP 6 in Phase 1 (aggradation of +0.4 m) and KP 5 in Phase 2 (aggradation of +0.9 m). At PDR, irregular riverbed aggradation occurs between KP 48 and 52 in Phase 1 (maximum aggradation of +2.4 m at KP 51), and between KP 63 and 66 in Phase 1 (maximum aggradation of +1.3 m at KP 64), and between KP 50 and 53 in Phase 2 (aggradation of +1.6 m). At MON, the entire reach exhibits riverbed incision in Phase 1 (−1.28 m average incision), whereas Phase 2 is associated with a stable bed elevation, with localized areas along the reach showing slight aggradation (ranging from −2.1 m incision to +2 m aggradation). At DZM, during Phase 1, aggradation is observed between KP 187 and 197 (maximum of +2.1 m at KP 193), slightly upstream of and at the confluence with the Ardèche River, whereas very slight riverbed incision occurs over the rest of the reach. In Phase 2, incision prevails, even at the confluence with the Ardèche River. Localized bed incisions downstream of the bypassed

https://doi.org/10.5194/egusphere-2026-3582
Preprint. Discussion started: 10 July 2026

reach, where the watercourse returns to its original course, are noteworthy (*e.g.*, maximum incision of −5 m at KP 197 in Phase 2 at DZM; see **Fig. 6B**).

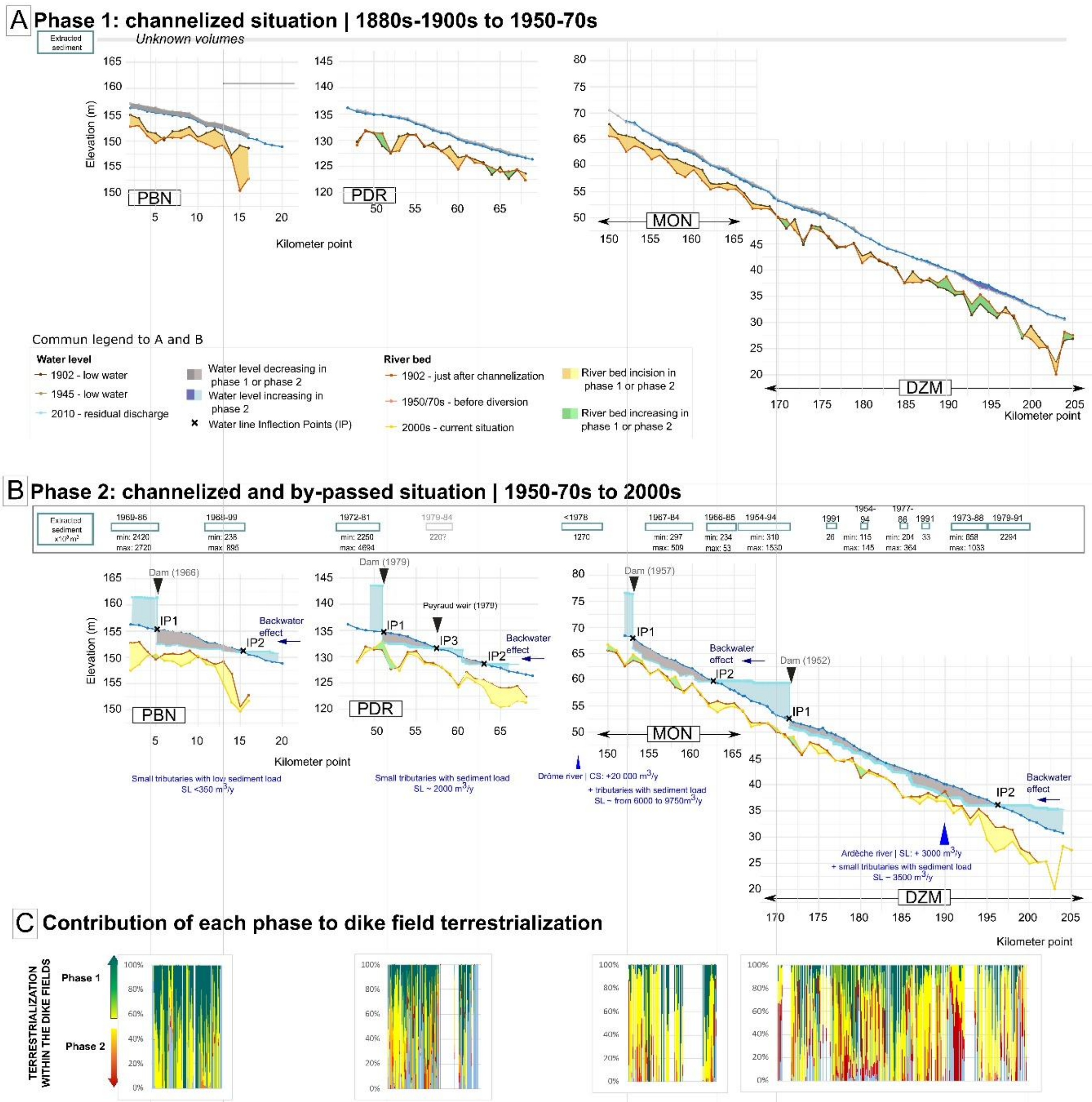

Fig. 6: Upstream–downstream overview of the changes in the water level and riverbed elevation during Phases 1 (A) and 2 (B). The water level surveys were conducted at specific periods: during the construction of the dike fields at low water levels (1902), prior to the implementation of the bypass during low water (1945), and for minimum flow conditions (20 m3·s⁻¹ in 2010). Riverbed surveys were carried out approximately 50–70 years after channelization and a few years after flow diversion, except for PDR, where the survey was conducted prior (as per Parrot et al., 2015). (C) Contribution of each time window to the dike field terrestrialization (percentage of terrestrial areas [TA%] within the dike fields; colors symbology according to the legend of Erreur ! Source du renvoi introuvable.**B.**

Due to their potential to induce riverbed incision, the gravel volumes extracted from the channel during Phase 2 have been located on the upstream–downstream gradient in *Erreur ! Source du renvoi introuvable.***A** and **B**. It is noteworthy that extractions are observed throughout the linear span of all four studied reaches. In addition, the annual coarse sediment volumes originating from major tributaries at the upstream level or within the reaches themselves are specified. During the discussion, we will revisit potential hypotheses regarding extraction location and volumes and incision trends.

4.2.2. Impact of the development phases on water levels

Comparing water levels is less conclusive when historical readings stem from exceptional low-water conditions, while current measurements represent an average situation corresponding to the residual flow passing through the Rhone bypass. Nevertheless, comparing the waterlines of 1902 and 1945 (Phase 1), both during low-water periods, provides a means of verification. It appears that PBN, the most incised reach, exhibits a lowering of the water level (−1.03 m; see difference shown in dark gray in **Figure 6A** – PBN) relative to others where the trend is barely noticeable or nonexistent.

During Phase 2 (**Fig. 6B**), the evolution of water levels before and after dam installation reveals, for each reach, noticeable changes in both waterline elevation and slope. In all cases, the first "space-time" inflection point (IP1) coincides with the location of the dam infrastructure. This pattern produces a flattening of waterlines both upstream and downstream of the dam, with a pronounced drop at the dam itself (−9.4 m at PBN, −10.9 m at PDR, −11.4 m at MON, and −9 m at DZM). The second "space-time" inflection point (IP2), located further downstream, corresponds to a sustained flat slope, reflecting the influence of the subsequent reservoir (see **Fig. 6B**, MON and DZM being consecutive).

4.2.3. Longitudinal gradients: coupled analysis of dike field terrestrialization and water level and riverbed change

Significant incision occurs at PBN during Phase 1 concurrently with substantial terrestrialization of its dike fields (see **Fig. 6C**, where the PBN map is particularly green). This is not the case at MON, where Phase 1 is characterized by a consistent incision trend along the entire upstream–downstream gradient, and the dike fields show little terrestrialization during this period. Terrestrialization following diversions (highlighted in yellow in **Figure 6C**) appears to correspond to gradients shaped by changes in water levels. Where water levels decrease (gray areas in **Figure 6B**), post-diversion terrestrialization (yellow areas in **Figure 6C**) is more pronounced; for example, between IP1 and IP2, except at PDR, where it occurs between IP1 and IP3 due to the influence of the weir. For example, the terrestrialized area increases by an average of 34.7% between KP 52 and 54, where emersion caused by the diversion is strongest on the PDR reach, compared with an average increase of 11.4% downstream between KP 55 and 61. In Phase 2 (**Fig. 6B**), where water levels rise—up to IP1 from the dam reservoir and down to IP2 from backwater effects (IP3 at PDR due to the Peyraud weir)— terrestrialization patterns and the proportion of water surfaces vary according to the position of the dike fields relative to these influences. It is difficult to identify general trends, and the GLMs attempting to explain terrestrialization through incision or dike field elevation changes do not yield clear patterns (insignificant p-values), likely due to insufficient data resolution. Nevertheless, these observations are corroborated by the manifestation of chrono-planimetric terrestrialization patterns and the residual areas of hydrological connectivity, which will be further explored in the following section.

https://doi.org/10.5194/egusphere-2026-3582
Preprint. Discussion started: 10 July 2026

4.3. Terrestrialization trajectories and residual lateral connectivity of alluvial margins

A synthetic overview of the dike fields—their average elevation, chrono-planimetric pattern, and terrestrialization percentage—in relation to recorded changes in water levels and riverbed evolution is provided in the **Appendix A, Figure 1**. This visualization reinforces the previously described trends: an upstream PBN reach with "perched" margins and an incised riverbed; PDR with margins close to the waterline and more contrasted terrestrialization rates; MON with a low density of dike fields that became strongly disconnected after diversion; and DZM, combining highly disconnected closed fields with open fields still connected at the water surface. It also suggests that the resulting terrestrialization pattern is strongly conditioned by the vertical position above the water level, which governs submersion frequency, as previously shown by Seignemartin et al. (2023).

At the reach scale, the frequency of overflow-driven lateral submersion—a proxy for hydrological connectivity over the past decades (post-diversion)—is estimated through modeling as 62 ± 121 $d \cdot y^{-1}$ at PBN, 87.2 ± 126.4 $d \cdot y^{-1}$ at PDR, 26.4 ± 73 $d \cdot y^{-1}$ at MON, and 70.6 ± 137 $d \cdot y^{-1}$ at DZM. The pronounced intra-reach variability underscores substantial differences in current hydrological connectivity, largely shaped by the local context of the dike fields. Despite this variability, MON consistently exhibits dike fields that have been markedly less hydrologically dynamic in recent decades compared with those in the other reaches, irrespective of dike field type (see **Appendix A, Figure 2**).

The current percentage of terrestrialized surface is strongly anticorrelated with the overflow-driven lateral submersion frequency of the dike fields ($D^2 = 0.74$, $p < 2.2 \times 10^{-16}$, obtained through a permutation test). The lower the submersion frequency, the more terrestrialized the dike fields are. However, concentric patterns deviate from this relationship, particularly for PDR and DZM (**Fig. 7**). These concentric patterns, typically situated outside the main data cluster, represent closed dike fields that are less terrestrialized than predicted. They exhibit lower terrestrialized surface percentages despite having submersion frequencies that would typically be associated with fully terrestrialized dike fields. When excluding the concentric patterns, the linear regression coefficient of determination increases to 0.90. In addition to the concentric pattern deviation, an abnormal distribution of residuals is observed for certain lateral patterns, where terrestrialization is either overestimated or underestimated.

https://doi.org/10.5194/egusphere-2026-3582
Preprint. Discussion started: 10 July 2026

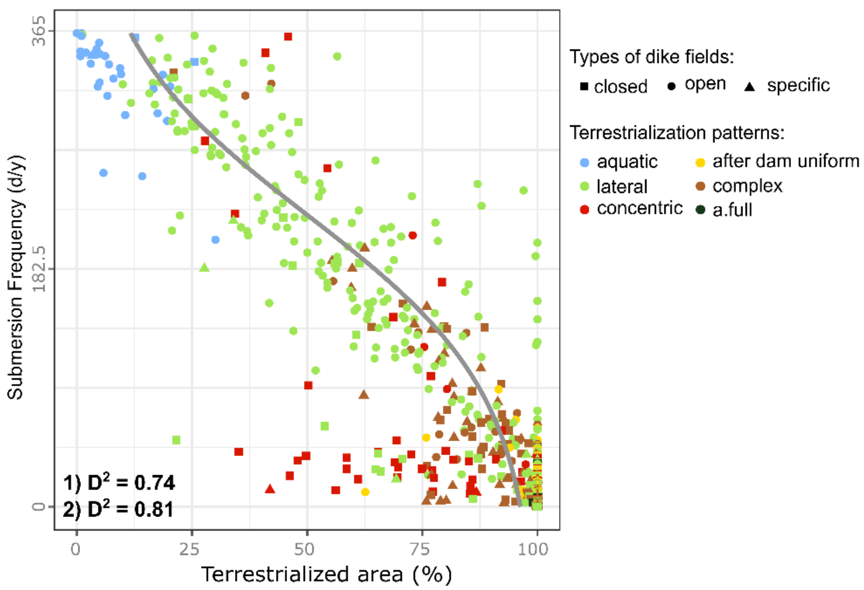

Fig. 7: GLM outcome illustrating the relationship between overflow-driven lateral submersion frequency and terrestrialization percentages across all reaches, where (1) D2 is calculated for the entire dataset, and (2) D2 excludes concentric patterns

The overflow-driven lateral submersion frequency model does not account for the hydraulic constraints or vegetation encroachment effects acting on the terrestrialization of engineered margins. As such, it offers a broad perspective but fails to capture local variations. This limitation is supported by the observed minimum dike relative elevations above the channel shown in **Appendix A, Figure 3**, which are lower for concentric patterns (e.g., longitudinal dike minimum at PDR = 1.25 m, IQR = 1.44) than for other patterns. These reduced elevations may stem from water inlets that promote recurrent erosive processes.

5. Discussion

5.1. Inter-reach comparison of channel responses

5.1.1. From morphological changes to underlying processes and drivers

Regardless the reach studied, both channelization and diversion phases contributed to channel narrowing, terrestrialization of alluvial margins, and disconnection of side channels. Tena *et al.* (2020) also demonstrated significant channel retraction and a decline in the number of flowing channels on the Rhône River, leading to the evolution of local anabranching reaches into highly stable single-thread channels. Focusing on the engineered margins, terrestrialization is also substantial. These terrestrialization trajectories are well depicted by chrono-planimetric patterns classified into five types (**Fig. 4B**), highlighting recurrent sediment storage and erosion modalities. In Seignemartin et al. (2023), we observed correspondences between them and the seven deposition patterns established by Sukhodolov et al. (2002) from flume experiments and observations on the Elbe River. Although their classification is derived from the proportion of filling and depositional forms that indicate flow recirculation and sediment accumulation at a specific moment, our chrono-planimetric typology is not designed to emphasize local hydraulic controls. Instead, it clarifies the influence of major fluvial alterations and depicts the associated terrestrialization trajectories. Additionally, the planimetric approach for characterizing sedimentary deposits was previously validated using an integrative methodology that combines ground-penetrating radar and topographic data, depicting a spatiotemporal architecture that aligns chrono-planimetric patterns with geophysical characteristics (Seignemartin et al., 2023). In a regulated context, the in-dike fine sediment deposits are shaped by residual shear stresses, which depend on the water discharge modalities of regulation (residual discharge versus flood or technical release), morphological context (such as relative elevation to the water level, concavity/convexity positioning), and the dike field characteristics, such as the type of structures (open/closed), as well as dike height (Räpple, 2018; Seignemartin, 2020). Additionally, the state of the dikes themselves is crucial for how shear stresses manifest and shape the deposits. A LiDAR DEM analysis has revealed that low points in the longitudinal dikes of closed fields form breaches, permitting water ingress (**Appendix A, Figure 3**). This results in circulating flows and scour patterns, which in turn create concentric sediment patterns and associated water ponds (Seignemartin, 2023). Intra-pattern variability could benefit from a localized hydraulic approach, offering insights into shear stress that shapes sediment deposition. GIS data could be combined with hydraulic models, such as those developed by Copeland (1983), Sukhodolov *et al.* (2002), and McCoy (2006). For example, the positioning of scour holes within groin fields (many in the lateral type) might be attributed to flow separation at the groin crests, which accelerates the flow near the groin's neck, shaping the sediment deposits (Sukhodolov, 2014).

Although both engineering works deeply modified the river landscape, the impacts of channelization and diversion dam phases vary across sites. In terms of side channel retraction, the impact of channelization predominates at PBN and MON, while it is somewhat more balanced at DZM. At PDR, we even observed an expansion of the water surface in Phase 2. In terms of main channel retraction, channelization predominates at PBN and PDR, whereas diversion has a greater influence at MON and DZM. Regarding terrestrialization, Phases 1 and 2 have an equivalent impact at PBN. Terrestrialization is slightly stronger in Phase 2 at PDR, whereas the diversion dam phase has a greater influence at MON and DZM. Although total terrestrialized area is highest at DZM and MON, the contributions of each phase vary: Phase 1 dominates at PBN and PDR, whereas Phase 2 plays a larger role at MON and DZM. Intensity metrics further highlight site-specific dynamics, with PBN exhibiting the highest rate during Phase 1 and DZM exhibiting the highest during Phase 2. These varied impacts can be discussed by examining how reaches adjust under the influence of four identified drivers that can promote either the accumulation of fine sediments (PROCESS 1) or the reduction of water flow (PROCESS 2).

https://doi.org/10.5194/egusphere-2026-3582
Preprint. Discussion started: 10 July 2026

5.1.2. In-dike sediment accumulation and deposit progression (PROCESS 1, DRIVER 1)

The four reaches experienced sediment accumulation in Phase 1 (PROCESS 1), leading to the progression of deposits (both lateral and vertical accretion) in closed fields, which is typical of fine sediment trapping due to the protection provided by longitudinal dikes (DRIVER 1). In the absence of these longitudinal dikes, terrestrialization is much less pronounced in open fields in Phase 1. Regarding the capacity of dike fields to trap sediments, the size of the structures (i.e., the distance between groins and the length of the groins) is key, as it controls the hydraulic constraints and patterns of sediment deposition (Copeland, 1983; Sukhodolov et al., 2002; McCoy, 2006). At DZM, the difference could be attributed to the larger dike fields and thus greater hydraulic constraints. At MON, the lower dike field density could explain the lower channel narrowing. Trends related to each driver and process are summarized in **Table 6**.

Table 6: Impact of different drivers on the processes leading to terrestrialization and alluvial disconnection across the four reaches.

		PBN	PDR	MON	DZM
PROCESS 1: fine sediment accumulation	**DRIVER 1: dike fields creating areas with reduced shear stress in phase 1 and 2**	**Phase 1:** Strong terrestrialization from sediment deposit accretion	**Phase 1:** Effective, but moderate impact in water surface loss of still important erosive processes	**Phase 1:** Effective, but low impact probably because of still important erosive processes (low dike field density).	**Phase 1:** Effective, but moderate impact probably because of still important erosive processes (larger and longer dike structures)
		Phase 2: Effective, but moderate impact on water surface loss. ➔ Vertical accumulation (high sediment thicknesses of PBN deposits (Räpple, 2018))	**Phase 2:** Cumulative impact with Driver 3 and Driver 4 leading to decreased shear stresses in the dike field and enough terrestrialization with remaining water areas.	**Phase 2:** Cumulative impact with Driver 3 leading to decreased shear stresses in the dike field and strong terrestrialization.	**Phase 2:** Cumulative impact with Driver 3 and Driver 4 leading to decreased shear stresses in the dike field and strong terrestrialization.
PROCESS 2: decrease in water levels leading to terrestrial emergence	**DRIVER 2: riverbed incision caused by the channelization in phase 1 + potential gravel extractions and depletion of tributary loads in phase 1**	**Phase 1:** Strong (mean incision: -2.11 m)	**Phase 1:** Low (mean incision: -0.27 m)	**Phase 1:** Moderate (mean incision: -1.28 m)	**Phase 1:** Null (+0.08 m)
	DRIVER 3: changes in water discharge due to diversion in phase 2	**Phase 2:** Effective, but moderate impact in water surface loss because dike fields are	**Phase 2:** Effective, and strong impact in water surface loss because of the drop in water level that disconnected the margins which was	**Phase 2:** Effective, and very strong impact in water surface loss because of the drop in water level that disconnected the	**Phase 2:** Effective, and strong impact in water surface loss because of the drop in water level that disconnected the margins which was

https://doi.org/10.5194/egusphere-2026-3582
Preprint. Discussion started: 10 July 2026

		already very disconnected	moderately terrestrialized	margins which was lowly terrestrialized	moderately terrestrialized
	DRIVER 4: riverbed incision caused by gravel extraction + potential depletion of tributary loads in phase 2	**Phase 2:** Strong (mean incision: -1.94 m)	**Phase 2:** Low to moderate (mean incision: -0.8 m)	**Phase 2:** Null (mean incision: -0.01 m)	**Phase 2:** Low to moderate (-0.64 m)

5.1.3. Effect of flow concentration on riverbed and water levels (PROCESS 2, DRIVER 2)

Regarding DRIVER 2, antagonistic phenomena are observed. Channelization concentrates the flow into a single-thread channel, which tends to physically raise water levels (Ghaffarian et al., 2021). However, the elevation of the waterline depends not only on discharge but also on changes in riverbed elevation. As discharge increases, shear stress also increases, often resulting in bed erosion and subsequent incision. If incision is significant, this compensatory effect can lower water levels and ultimately trigger the emergence of terrestrial areas (PROCESS 2). At PBN, which has the highest density of dike fields concentrating shear stress within the main channel, the most substantial riverbed incision occurs during Phase 1. All four reaches show varying degrees of riverbed incision; however, the effect on water levels could not be verified because the test was not significant, likely due to the limited resolution of the water level dataset and differing flow conditions. The absence of data on sediment extraction during the first half of the 20th century prevents determining whether sediment extraction may have contributed to sediment starvation and riverbed incision during this period.

5.1.4. The "backwater effect" of diversion dam series on water level (PROCESS 2, DRIVER 3)

Significant changes in waterlines for each reach (DRIVER 3) have been highlighted through comparisons before and after dam construction, affecting both water levels and slopes. Each reach presents a first "space-time" inflection point (IP1) where pre- and post-dam water level representations cross (**see Fig. 6**). It corresponds to the dam infrastructure, resulting in a flattening of the regulated water level both upstream and downstream of the dam, with a step change of several meters at the dam drop. The second "space-time" inflection point (IP2), downstream of the reaches, shows that the slope of the regulated water level does not recover and remains flat, influenced by the subsequent downstream reservoir (backwater effect). This phenomenon is characteristic of configurations with bypassed series, emphasizing that even outside of developments, their effects are observed. Their spatial footprint extends well beyond the dam location, affecting a substantially larger river reach and not solely through indirect impacts. In summary, the longitudinal gradient of water levels within the bypassed reaches is influenced by both dams and backwater effects, as well as weirs where present (e.g., Peyraud weir at PDR). Consequently, the connectivity between the channel and its margins varies over time and space along this upstream–downstream gradient. This is an additional factor that may explain intra-reach/local variability in terms of chrono-planimetric and semi-aquatic patterns.

https://doi.org/10.5194/egusphere-2026-3582
Preprint. Discussion started: 10 July 2026

5.1.5. Dam and associated sediment extraction effect on channel long profile (PROCESS 2, DRIVER 4)

Regarding the evolution of the riverbed following dam construction, typical adjustments include riverbed aggradation upstream of the dam and post-dam incision. The former is caused by the dam reservoir, which creates conditions for sediment accumulation, while downstream, constraints due to unreduced flow lead to incision tendencies (Kondolf, 1997; Ibisate et al., 2013). The pattern of riverbed aggradation upstream of the dam is observed at PDR and MON but not at PBN and DZM (see **Erreur ! Source du renvoi introuvable.B**). These two reaches underwent significant gravel extractions (DRIVER 4) concomitant with dam construction (see incision pattern and gravel pit location in Erreur ! Source du renvoi introuvable.**B).** This highlights that dams affect the river not only by altering the channel but also by depleting alluvial deposits through gravel extractions carried out during construction. Cœur *et al.* (2017) assessed the maximum volumes of coarse sediments extracted, which were variably distributed over time in Phase 2 and localized, rather than uniform across the reaches (see **Fig. 6B**). The total extraction was 3.9 million m³ during Phase 2 at PBN, primarily due to dam construction and management adjustments in the 1970s and 1980s. At PDR, the total extraction reached 6.6 million m³ during Phase 2, whereas 3.3 and 6 million m³ were extracted at MON and DZM, respectively. Moreover, even in reaches that did not experience significant riverbed incision, such as DZM, the riverbed aggradation observed during Phase 1 at KP 190, near the confluence with the Ardèche River, is no longer visible in Phase 2. Instead, a decrease in riverbed elevation is observed, likely due to insufficient sediment supply in a context of overall sediment depletion.

Furthermore, it is generally expected that flow reduction in the bypassed reach would decrease in-channel shear stress and mitigate incision trends, as observed in a bypassed section of the Old Rhine (Arnaud et al., 2015), and similarly at PDR (Seignemartin et al., 2023). However, despite the reduced shear stresses following flow diversion, initially exacerbated by channelization in the “old” channel, the riverbed continues to incise locally to varying degrees around gravel extraction sites, likely influenced by the site-specific local hydromorphological conditions.

5.1.6. The hydromorphological legacy of Phase 1 on Phase 2

In the reaches less affected by Phase 1, more significant adjustments occurred following the diversion. At PDR, the greater contribution of Phase 1 compared with Phase 2 in channel narrowing is not associated with a particularly substantial post-channelization riverbed incision. This Phase 1 dominance may result from (i) data limitations, such as low discharge on the “pre-diversion” reference date, which increased contrast in Phase 1 but reduced it in Phase 2, or (ii) higher hydrological connectivity in the margins, due to lower dikes and more breaches or concentric patterns, leading to variable connectivity and reduced terrestrialization in Phase 2. In Phase 2, channel retraction and dike field terrestrialization are dominant at MON and DZM, while the processes of incision and fine sediment accumulation from Phase 1 were actually less pronounced.

https://doi.org/10.5194/egusphere-2026-3582
Preprint. Discussion started: 10 July 2026

5.1.7. Cumulative impact of multiple dams on sediment transfer

Vázquez-Tarrío *et al.* (2019) demonstrated that a series of multiple dams can have a cumulative impact on sediment transfers and geomorphic interactions between successive reaches. PBN is the first reach in the upstream–downstream gradient, with PDR being the second; MON and DZM are respectively the seventh and eighth in the series downstream of Lyon. Due to channelization, in-channel shear stresses and transport capacity increased during Phase 1. Consequently, the riverbed of the most upstream channelized portion would experience incision (as observed at the PBN reach, see **Fig. 6**). Through a cascade effect, downstream reaches may benefit from the sediment load supplied by upstream channelized sections, which could explain the moderate bed incision observed in intermediate reaches such as PDR and the highest incision observed at PBN.

5.2. Temporal trends in engineered margins

5.2.1. Channelization-induced terrestrialization

The impact of dike field construction in the late 19th and early 20th centuries included a reduction of water surface areas and accelerated terrestrialization by concentrating flow, which led to channel incision, upstream narrowing, and the disconnection of numerous side channels (Phase 1 in **Fig. 8**) (Roux et al., 1989; Parrot, 2015; Riquier, 2015; Räpple, 2018; Tena et al., 2020; Seignemartin et al., 2023). Diachronic planimetry confirms that the phenomenon followed a distal-to-proximal sequence: the farther the side channels were from the main channel, the less hydrologically connected they remained, and the more they underwent terrestrialization. Where their connection was affected by dikes, these side channels experienced an even more pronounced loss during the first phase of channelization (Roux et al., 1989; Riquier et al., 2015). After affecting the side channels (Citterio and Piégay, 2009; Riquier et al., 2017), terrestrialization subsequently affected the distal sections of the dike fields (Phase 1) and eventually reached the proximal areas of the dike fields (Phase 2). Terrestrialization was further enhanced by sediment deposition, which depended on several factors, including hydrological connectivity influenced by embankment configurations, local hydraulic constraints, and the progressive disconnection caused by corrective measures (i.e., the density and size of dike fields relative to each reach). During Phase 1, discharge was not diverted, and shear stresses along the margins remained high, preventing significant sediment accumulation. It was primarily along the outer edges of highly protected, closed dike fields and disconnected side channels that fine sediments accumulated, initiating the early stages of vegetation encroachment.

https://doi.org/10.5194/egusphere-2026-3582
Preprint. Discussion started: 10 July 2026

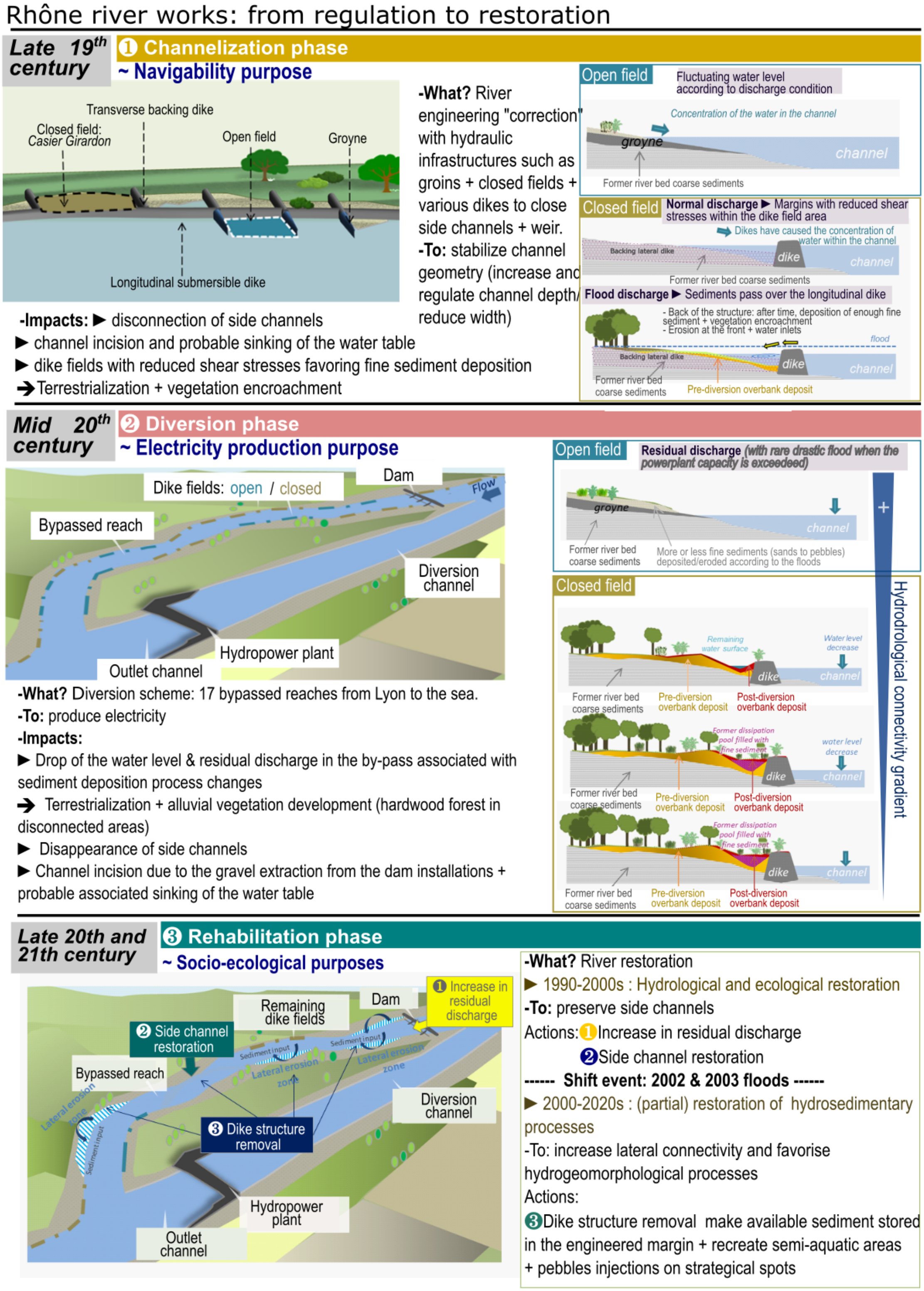

Fig. 8: Phases of development and evolution of the Rhône: from anthropization to socio-ecological rehabilitation

https://doi.org/10.5194/egusphere-2026-3582
Preprint. Discussion started: 10 July 2026

5.2.2. A terrestrialization sustained by diversion dams

The implementation of diversions (Phase 2 in **Fig. 8**) caused a direct reduction in water areas in the bypassed reach by diverting the majority of water discharge into the hydroelectric side canal, resulting in long-lasting changes to water levels and slopes and inducing a regulated flow regime. Initially intense, the terrestrialization response to the dam is succeeded by an asymptotic relaxation, consistent with post-dam adjustments described by Graf (1977), Surian and Rinaldi (2003), Petts and Gurnell (2005), and Arnaud *et al.* (2015). After dam construction, water discharge is reduced and regulated, and significant surface emersion is observed (yellow areas in Erreur ! Source du renvoi introuvable.**B** and typical patterns such as uniform after-dam patterns). During the relaxation sequence, although terrestrialization and associated disconnection promote vegetation encroachment (Seignemartin, 2020), the increased roughness from vegetation can also modify hydrodynamics and exacerbate sediment accumulation (Arnaud et al., 2015; Sukhodolov et al., 2017). Consequently, the storage of fine sediments in dike fields is favored by a reduction in average erosive processes due to the protection provided by the dike fields, vegetation encroachment, and the regulated discharge regime (except during significant flood events that release water into the original channel). The aggradation and stabilization of sediment deposits further disconnect the river channel from its "perched" alluvial margins. These margins, still constrained by the dike fields, become even less hydrologically connected and, as a result, more prone to store fine sediments that are unlikely to be remobilized. Indeed, even during floods, closed fields can be submerged but the established alluvial forest vegetation helps retain deposits (Räpple, 2018). When floodwaters recede, longitudinal dikes trap sediments, resembling classic overbank sedimentation patterns (e.g., Middelkoop and Van Der Perk, 1998), which is confirmed by field observations showing fine sediment accumulation within closed fields, often marked by deposits around trees. In contrast, open fields display greater variability. Without the protection of a longitudinal dike, their morphological dynamics are primarily controlled by their configuration (e.g., submerged or sloping groins), their position relative to the main channel, and local hydraulic conditions. Less dynamic open fields support pioneer herbaceous and shrubby vegetation and accumulate fine sediments, whereas more dynamic areas display mineral surfaces (pebble banks) where vegetation does not establish.

5.2.3. Effects of diversion regulation on hydrological connectivity

Dams induce hydrosedimentary impacts across space and time. Dams trigger immediate transformations through site associated engineering works such as levees, canals, islands, hydraulic dredging, and channel reconfiguration (Phase 2 in **Figure 8**). In the short to medium term, river reaches undergo rapid adjustments, including terrestrialization and vegetation encroachment following flow diversion. Over the longer-term, changes emerge in morphogenic sediment dynamics, fine sediment accumulation, and the development of hardwood forest, among other processes. Among these alterations, one of the most significant is the modification of hydrological connectivity. This connectivity plays a key role in regulating water-mediated exchanges, with flood disturbances being essential for maintaining habitat diversity, supporting biodiversity, and sustaining overall alluvial ecological functions and processes (Amoros and Wade, 1996; Tockner et al., 1999; Geerling et al., 2006). The dam-induced alteration of hydrological connectivity led to formation of engineered terrestrial margins and shaped a threshold-controlled floodplain, where inundation occurs only when the discharge capacity of the hydropower plant is exceeded.

5.2.4. A multi-factor–driven riverbed incision, amplifying the disconnection of margins

The riverbed experienced varying degrees of incision, primarily due to increased transport capacity and sediment starvation at the reach scale (Roux, 1989). During Phase 1, shear stress is concentrated within a single channel. Although hydraulic forces decreased in Phase 2, as most of the flow was diverted into the side canal, bed incision continued in the original channel, further exacerbated by sediment extractions associated with dam construction and sediment trapping at tributary confluences to prevent navigation problems. In some cases, incision could exacerbate the water level decline, further amplifying floodplain disconnection (Scott et al., 1999; Arnaud et al., 2012; Parrot, 2015). This is particularly evident in the case of most upstream study reach (PBN), where the vegetation is characteristic of disconnected environments, featuring secondary succession hardwood species (Janssen et al., 2020).

5.3. Comparison with other modified European rivers

The Rhine and Danube experienced extensive 19th- and 20th-century engineering works that profoundly altered their morphology and ecological systems (Hohensinner et al., 2004; Arnaud et al., 2015, 2019; Habersack et al., 2016). The Upper Rhine, once a braided and anastomosed river, underwent extensive channelization beginning in the 19th century, with levees constructed to mitigate flood risk. Groins were added in the 1930s, followed by major dam construction in the 1950s, which further modified flow and sediment dynamics. In the Danube's Machland region, river straightening began in the 19th century, followed by dam and levee construction in 1957. Pumping stations were later installed to manage groundwater levels and the floodplain system.

Extensive human interventions in the Po River—including navigation works utilizing cobbles and stone slabs for bank protection, the construction of groins in the 1930s and 1940s, and sediment extraction activities in the 1960s and 1970s—led to a transition from an anabranching or wandering river system to a sinuous, single-thread configuration (Brenna et al., 2022, 2024).

5.3.1. Channelization phase contribution to river geomorphic changes

On the Rhine reach, channelization led to an average reduction of −67% in active channel width, compared with a −49% reduction on the Danube and between −17% and −40% on the Rhône (data for the Po River are unavailable) (Table 7). In terms of intensity over time, channelization shows an average retraction rate of −10.9 $m \cdot y^{-1}$ on the Rhine, −2.4 $m \cdot y^{-1}$ on the Danube, and between −0.5 and −1.5 $m \cdot y^{-1}$ on the Rhône (Table 7). The average bed incision associated with channelization is −7 $cm \cdot y^{-1}$ for the Rhine reach (total average incision: −5.3 m), unknown rate for the Danube reach (with an estimated average incision of −1.7 m), and ranges from −3 to +0.2 $cm \cdot y^{-1}$ for the Rhône (total average incision: ranging from −2.1 m to no

https://doi.org/10.5194/egusphere-2026-3582
Preprint. Discussion started: 10 July 2026

incision) (Table 7). Channelization generally exerts a more pronounced effect on bed incision, particularly in the Rhine and Danube rivers, where it leads to substantial riverbed degradation over time. The Rhône, in particular, displays a wide range of responses to diversion across different reaches, with some areas experiencing notable incision, whereas others remain stable or show slight aggradation.

Therefore, channelization led to a loss of alluvial forms, narrowing of both main and side channels, and, in most cases, the transition of active secondary channels into disconnected channels that eventually fill in and disappear. The magnitudes of reduction are of the similar order across rivers but show variations that may be attributed to differences in infrastructure—such as density, type, and location—as well as to each river's specific response to these modifications. Potential bias may also arise from differences in the initial extent of side-channel areas, which depend on the type of planform pattern initially present in each river system.

https://doi.org/10.5194/egusphere-2026-3582
Preprint. Discussion started: 10 July 2026

Table 7: Characteristics of other rivers affected by channelization, diversion, or gravel mining and the associated.

Studied water body	Rhine	Po River	Danube	Rhône River
Source/study	Arnaud *et al.*, 2019 Arnaud *et al.*, 2015	Brenna *et al.*, 2022 Brenna *et al.*, 2024	Hohensinner *et al.*, 2004	*See results of this study*
Location	France (Upper Rhine)	Italy (Middle Po)	Austria (Machland region)	France (Middle Rhône)
Period covered by the study	1828 to 2009	1930s to 2008	1812 to 1991	1880s to 2009
River type before engineering works	Braided and anastomosed channel	Multi− thread configurations	Island− braided	Braided channel
Engineering phases	1. 19th− century channelization: dikes (levees) constructed over 600 to 900m longitudinal sections with 50− m long intervals between section and high− flow dikes several hundred meters behind the channelized river. 2. 1930s: lateral groyne construction 3. 1950s damming and by− passing	1. 1930s− 1950s: Training scheme for navigation: elongated bent structures using cobbles and stone slabs for bank protection and groynes 2*. 1960s− 1970s: Sediment and water resource exploitation	1.19th− century channelization/river “straightening” 2. Damming and by− passing (1957) + associated artificial levees + pumping stations at the confluences of two dominating backwater systems to the main channel, drain the floodplain for the purpose of lowering the groundwater table.	1.19th− century channelization/river “correction” with closed and open fields 2. Damming and by− passing (1950s− 1970s) + gravel extraction
Approach & data sources	Planform changes from historical maps, aerial photographs and satellite image Topographic changes from longitudinal profiles and cross sections	Planform changes from historical maps, aerial photographs and satellite image Topographic changes from cross sections	Planform changes from historical maps Topographic changes via information on historical maps (terrain heights, characteristic water levels)	Planform changes from historical maps, aerial photographs and satellite image Topographic changes from longitudinal profiles and cross sections, historical water level datasets
Extent of the studied reach	50− km long reach on the Upper Rhine between Kembs & Breisach	123 km subdivided in 10 reaches from 7.6 km to 17.5 km between the confluence of the Adda River (near the Isola Serafini Dam) and Secchia River	10.25 km long reach → Head of the reservoir of the power plant Ybbs− Persenbeug	4 reaches Cumulating 60 lkm
Example of quantified geomorphological changes				
	Active channels (main channel + side channels)			
Median active channel retraction (width in meter)	**P1:** 1828–1925: − 67%, from 902 to 302 m **P2:** 1925− 2008: − 12% from 302 m to 111 m	**P1:**1930s− 1950s: unknown **P2*:**1954− 1998: ~− 20% on the upper reaches e.g., from 559 to 448 m (B2 section) ~ − 50% retraction on the reaches marked by severe incision; e.g., from 680 to 375 m (F1 section) **After P2*:** 1998–2020: average narrowing ~ − 7%, e.g., from 375 to 329 m (F1 section)	**P1:** 1812–1925: − 49%, from 560 to 286 m** **P2:** 1925− 1991: − 2%, from 286 m to 274 m**	**MAIN + SIDE CHANNELS → “ACTIVE CHANNELS** **P1:** 1860–1950s/70s: Max − 43 % (PBN) to min − 17% (DZM), PBN: from 346 to 199 m & DZM: from 278 to 231m **P2:** 1950s/70s− 2000s: Max − 32% (MON) to min − 17 % (PDR), MON: from 254 m to 172 m & PDR: from 208 m to 172 m
Associated rate of active channel retraction (m yr− 1)	**P1:** 1842–1872 rate: 10.9 m yr− 1 **P2:** 1956–2008: 1.3 to 0.1 m yr− 1	**P2:** 1954–2008: 7.3 m yr− 1 **After P2*:** 1998–2020: 2.1 m yr− 1	**P1:** 1812–1925: 2.4 m yr− 1 **P2:** 1925− 1991: 0.2 m yr− 1	**P1:** 1860–1950s/70s: Max − 1.6 m yr− 1 (PBN) to min − 0.5 m yr− 1 (DZM), **P2:** 1950s/70s− 2000s: Max − 1.3 m yr− 1 (MON) to min − 0.9 m yr− 1 (PDR),
Average change (on the reach length) in river bed elevation (m) River bed elevation ($cm \cdot y^{-1}$)	**P1:**1880–1950: ~ − 5.3 m; i.e., − 7 $cm \cdot y^{-1}$ **P2:**1950–2009: ~ − 2.4m; i.e., − 0.4 $cm \cdot y^{-1}$	**P1:**1930s− 1950s: bed stability. **P2*:**1954− 1969: in sections without groynes; average incision − 1 to − 3 m; i.e. from − 7 to − 20 $cm \cdot y^{-1}$ Up to − 7m (− 47 $cm \cdot y^{-1}$) Stability or deposition in sections with groynes **After P2*:**1980s – 2000s: limited changes	**P1:** beginning of the 20th century: river bed incised by up to − 1.7 m **P2:** mid− 19th century: Proxy: − 1.4 m in groundwater table elevation in the Machland floodplain	**P1:**1860–1950s/70s: ~ from − 2.1 m to +0.1m; i.e., from − 3 $cm \cdot y^{-1}$ (PBN Reach) to +0.2 $cm \cdot y^{-1}$ (DZM reach); **P2:**1950s/70s− 2000s: ~ from − 4.1 m to 0 m; i.e., from − 5 $cm \cdot y^{-1}$ (PBN Reach) to null (MON reach)

the phase 2 here refers to gravel mining activities
**calculated from area data and reach length

https://doi.org/10.5194/egusphere-2026-3582
Preprint. Discussion started: 10 July 2026

5.3.2. Diversion cumulative contribution to river geomorphic changes

On the Rhine reach, diversion is associated with an average loss of −12% in bypassed channel width, compared with a −2% width reduction on the Danube and between −17% and −32% on the Rhône (with data unavailable for the Po River) (Table 7). In terms of intensity, diversion is associated with an average retraction rate of −0.1 to −1.3 $m \cdot y^{-1}$ for the Rhine, 0.2 $m \cdot y^{-1}$ for the Danube, and between −0.9 and −1.3 $m \cdot y^{-1}$ for the Rhône (Table 7). This places the Rhône as the river with the most significant reduction due to diversion impacts. On the Rhône, we also noted that reaches undergoing substantial retraction and terrestrialization due to channelization seemed to experience a less pronounced impact from diversion, whereas reaches less affected by channelization exhibited a stronger response to diversion. This explanation may also be applicable to the other rivers examined in the study, indicating that the initial impacts of channelization could be so pronounced that they obscure or diminish the geomorphological effects of subsequent diversion. This "masking effect" could stem from the reliance on broad, bimodal planform indicators of land occupation (aquatic versus terrestrial), which are typically aggregated at a reach scale. Such an approach may be too generalized to capture local− scale changes and the full range of land occupation dynamics (vegetation type, etc.). For diversion, the average bed incision is −0.4 $cm \cdot y^{-1}$ for the Rhine reach (total average incision: −2.4 m), unknown rate for the Danube reach (proxy: −1.4 m based on groundwater table elevation changes in the Machland floodplain), and ranges from −5 $cm \cdot y^{-1}$ to no incision for the Rhône (total average incision: ranging from −4.1 m to no incision). Variations in geomorphological responses may be attributed to differences in sediment dynamics, hydraulic conditions, and local factors such as sediment supply, channel morphology, infrastructure characteristics, and the spatial relationship between gravel extraction sites and dam constructions, all of which likely play a crucial role in shaping geomorphological dynamics.

5.3.3. Gravel extraction cumulative contribution to river geomorphic changes

On the Po reach, the rate of active channel retraction associated with the period of massive gravel extraction reached 7.3 $m \cdot y^{-1}$ (1954–2008), with an average retraction of 50% in the most affected areas. In contrast, the preceding period, limited to channelization initiated in the 1930s, experienced a more moderate narrowing of approximately 20%. This intense phase of retraction was followed by a relaxation phase in the 1990s and 2000s, when gravel extraction ceased. Nevertheless, retraction persisted, slowing to an average rate of 2.1 $m \cdot y^{-1}$ due to ongoing sediment depletion, exacerbated by the Isola Serafini Dam. Gravel extraction is also linked to substantial riverbed degradation, particularly in unprotected areas, where average incision depths reached 3 m, with some sites experiencing declines of up to 6–7 m. Conversely, groin− protected sections exhibited greater stability or even sediment deposition. Despite the pronounced retraction, the cumulative effects of channelization infrastructure contributed to stabilizing bed elevation, whereas unprotected areas continued to undergo incision and further narrowing. In the case of the Po, extractions strongly drive channel narrowing, which is not directly comparable to the more localized extractions on the Rhône; however, the focus here is not on that comparison but rather on highlighting the impact of channelization infrastructure, which in the Po limits incision, illustrating the concept of legacy− dependent sub− trajectories.

https://doi.org/10.5194/egusphere-2026-3582
Preprint. Discussion started: 10 July 2026

6. Conclusion

Channelization and flow diversion both play crucial roles in the terrestrialization and disconnection of the Rhône River alluvial margins. However, their impacts are not uniform, as they are influenced by the initial state of margin connectivity, local hydromorphological conditions, and cumulative environmental pressures. Channelization induces significant changes in fluvial morphology, as evidenced by planform studies, which reveal the transition from a multi− thread to a single− thread system.

Additionally, gravel extraction linked to dam construction challenges earlier assumptions. Despite reduced shear stress after flow diversion—previously intensified in the main channel by channelization—the riverbed continues to incise locally, particularly in extraction zones, with the degree of incision and expansion varying according to the specific hydromorphological context.

In areas where channelization strongly controlled terrestrialization, the additional influence of flow diversion remained relatively limited, illustrating legacy− dependent adjustment trajectories shaped by the system response to previous interventions. However, in reaches where channelization had less impact, the drop in water level caused by flow diversion drove substantial additional terrestrialization of channel margins.

One of the common syndromes of Anthropocene rivers is alluvial disconnection, and the history of the Rhône's modified margins reveals its complex dynamics, with dike fields acting as both agents and witnesses of terrestrialization. These dike fields also offer valuable insights into the remaining hydrological potential, thereby presenting opportunities for eco− morphological restoration and fluvial reconnection efforts.

as well as Robin Gruel, Bianca Räpple, Alvaro Tena, and Pierre− Hugo Lecomte for their contributions to fieldwork.

Appendix A

Table A1. Characteristics of the photograph series.

Year	Source	Reach	Date	Resolution	Photo type	Color type	Daily total Q (m3/s) | Residual Q when bypassed	Mission ID
1945	IGN	PBN	30/09/1945	1	Argentic	B&W	596	C94PHQ3871_1945
1954	IGN	PBN	26/05/1954	1	Argentic	B&W	558	C3032− 0061_1954
1973	IGN	PBN	01/01/1973	1	Argentic	B&W	364	C3032− 0311_1973
1993	IGN	PBN	16/08/1993	1	Argentic	Colour	464	C93SAA0982_1993
2008	IGN	PBN	02/05/2008	0.5	Numeric	Colour	1070	CP08000032_FD69
1938	IGN	PDR	17/08/1938	1	Argentic	B&W	877	C3410− 0221_1938
1949	IGN	PDR	01/10/1949	1	Argentic	B&W	342	C3031− 0551_1949
1974	IGN	PDR	26/07/1974	1	Argentic	B&W	510	C3033− 0201_1974
1979	IGN	PDR	20/06/1979	1	Argentic	B&W	1140	C2934− 0041_1979
1982	IGN	PDR	09/07/1982	1	Argentic	B&W	810	C3329− 0031_1982
1986	IGN	PDR	25/06/1986	1	Argentic	Colour	882	C2928− 0012_1986

1991	IGN	PDR	16/07/1991	1	Argentic	Colour	731	C91SAA2002_1991
2002	IGN	PDR	20/05/2002	1	Argentic	Colour	1200	CP02000012_2002
2009	IGN	PDR	04/06/2009	50 cm	Numeric	Colour	634	CP09000262_FD38F80
1946	IGN	MON	08/10/1946	1	Argentic	B&W	670	C3036− 0051_1946
1961	IGN	MON	29/06/1961	1	Argentic	B&W	1620	C2938− 0023_1961
1978	IGN	MON	31/05/1978	1	Argentic	B&W	2210	C3038− 0021_1978
1991	IGN	MON	16/07/1991	1	Argentic	Colour	731	C91SAA2002_1991
2007	IGN	MON	26/07/2007	50 cm	Numeric	Colour	1410	CP07000142_FD0007
1947	IGN	DZM	03/09/1947	1	Argentic	B&W	760	C2939_0041_1947
1954	IGN	DZM	13/05/1954	1	Argentic	B&W	1020	C2940_0101_1954
1955	IGN	DZM	15/03/1955	1	Argentic	B&W	1110	C2939_0031_1955
1976	IGN	DZM	19/06/1976	1	Argentic	B&W	490	C2939− 0011_1976
1994	IGN	DZM	29/04/1994	1	Argentic	B&W	2220	C94SAA0401_1994
2002	IGN	DZM	19/05/2002	1	Argentic	Colour	1030	P02000012_2002
2009	IGN	DZM	28/05/2006	50 cm	Numeric	Colour	1280	CP06000072_fd0026

Table A2. Comparative Root Mean Square Error (RMSE) values for the older and more recent series of photographs for each reach.

	Series	**N picture**	**RMSE (Mean ± SD)**
PBN	1947 series	6	5.3 ± 1.3
PBN	1993 series	4	4.1 ± 1.4
PDR	1938 series	6	4.1 ± 1.6
PDR	2002 series	5	2.2 ± 0.9
MON	1946 series	9	3.6 ± 1.8
MON	2001 series	4	2.3 ± 0.7
DZM	1947 series	19	1.8 ± 1.1
DZM	2002 series	13	2.4 ± 1.5

https://doi.org/10.5194/egusphere-2026-3582
Preprint. Discussion started: 10 July 2026

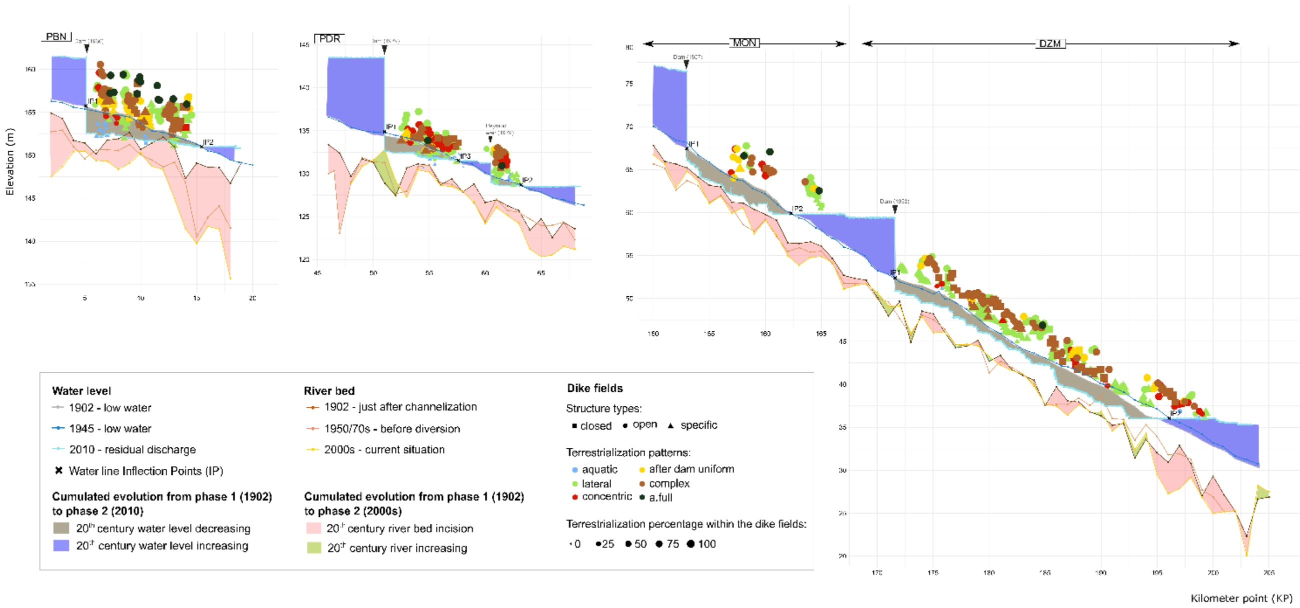

Fig. A1. Dike field situation along the upstream− downstream gradient after over a century of multi− pressure terrestrialization. associated with an overview of the water level and riverbed evolution.

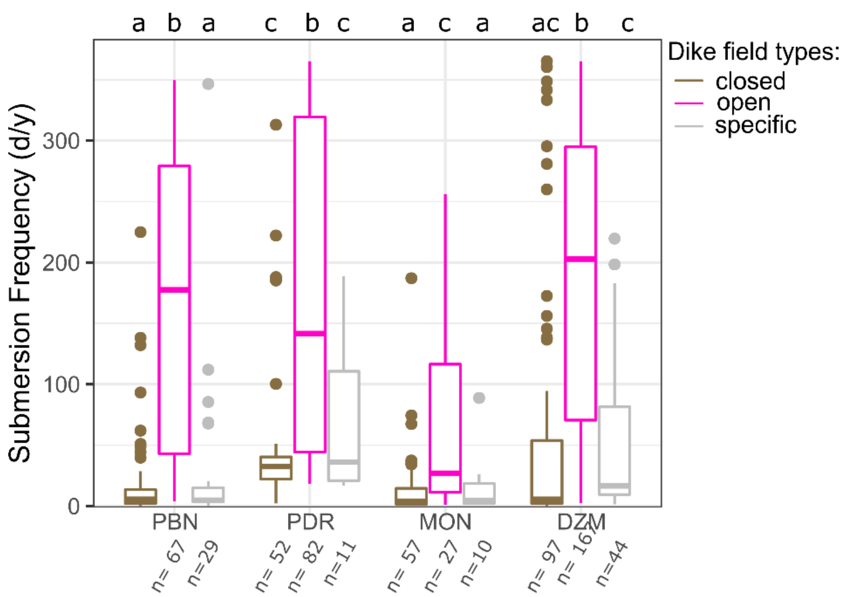

Fig. A2. Dike field overflow− driven lateral submersion frequency according to the dike field type and reach. Letters (a, b, c) denote homogeneous groups identified by pairwise Wilcoxon signed-rank tests. Groups sharing a letter are not significantly different (p > 0.05).

https://doi.org/10.5194/egusphere-2026-3582
Preprint. Discussion started: 10 July 2026

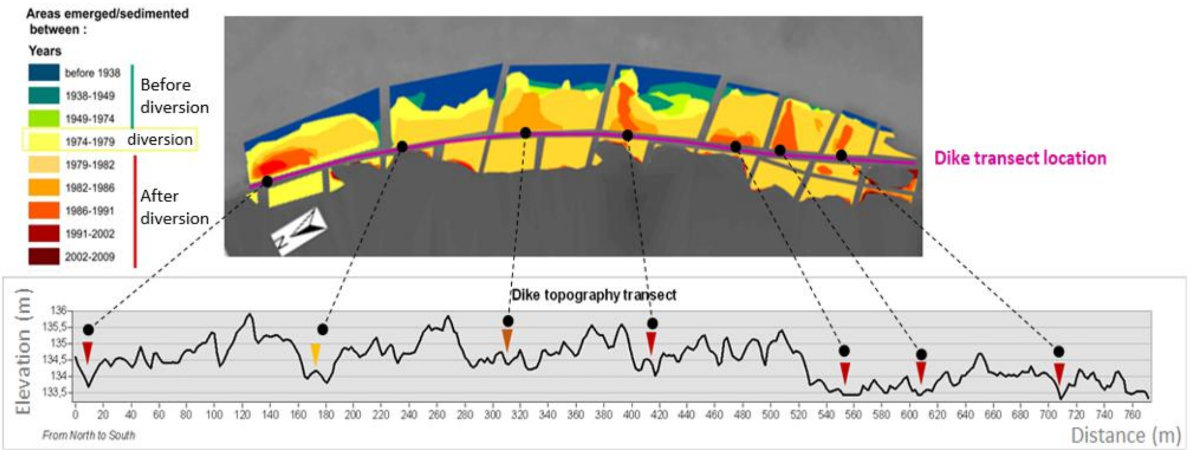

Fig. A3. Linking concentric patterns with low points identified along the topographic transect (extracted from LiDAR DEM collected by IGN in 2010) of the longitudinal dike of the closed field (PK 55, left bank of PDR).

Code and data availability

Analyses were performed using standard statistical and GIS software. No custom code was developed for this study. Part of the data used in this study originates from previously published datasets cited throughout the manuscript. Additional data generated and processed during the current study are available from the corresponding author upon reasonable request.

Author contributions

G. Seignemartin: Conceptualization; Data Curation; Formal Analysis; Investigation; Methodology; Software; Validation; Visualization; Writing – Original Draft; Writing – Review & Editing.

B. Mourier: Validation; Writing – Review & Editing.

J. Riquier: Writing – Validation; Review & Editing.

H. Piégay: Validation; Conceptualization; Supervision; Writing – Review & Editing.

Competing interests

The authors declare no competing interests.

Disclaimer

Copernicus Publications remains neutral with regard to jurisdictional claims made in the text. published maps. institutional affiliations. or any other geographical representation in this paper. While Copernicus Publications makes every effort to include appropriate place names. the final responsibility lies with the authors. Views expressed in the text are those of the authors and do not necessarily reflect the views of the publisher.

Acknowledgements

We thank the staff and partners of the EVS 5600 laboratory (UMR 5600, Environnement Ville Société, Université de Lyon – CNRS), including Mélanie Bertrand, Katarína Džubáková, Daniel Vázquez–Tarrío (members during the study period), as well as Robin Gruel, Bianca Räpple, Álvaro Tena, and Pierre-Hugo Lecomte for their contributions to fieldwork. We also acknowledge the staff of the LEHNA–IAPHY team (UMR 5023, Laboratoire d'Écologie des Hydrosystèmes Naturels et Anthropisés – Ingénierie et Aménagement des Phénomènes Hydrosédimentaires, Université Lyon 1 – CNRS), including Thierry Winiarski, Elie Dhivert, and André-Marie Dendievel (members during the study period or currently affiliated), for their support. AI-assisted tools were used to improve the English language during drafting. The authors take full responsibility for the scientific content. The final version was edited by Elsevier Language Editing Services.

Financial support

This study was conducted as part of the Rhône Sediment Observatory (OSR) program, a collaborative research initiative supported by the European Regional Development Fund (ERDF) through Plan Rhône, the Agence de l'Eau Rhône Méditerranée Corse, CNR, EDF, and the regional councils of Auvergne–Rhône–Alpes, Provence–Alpes–Côte d'Azur (PACA), and Occitanie. The research was carried out within the framework of the EUR H2O'Lyon program (ANR-17-EURE-0018) at Université de Lyon, funded through the French "Investissements d'Avenir" program managed by the French National Research Agency (ANR), with additional support from the LabEx DRIIHM (ANR-11-LABX-0010).

References

Acthys: Étude historique des prélèvements de sédiments dans le Rhône (1954–2010), 2017.

Amoros, C., and Bornette, G.: Connectivity and biocomplexity in waterbodies of riverine floodplains, Freshwater Biology, 47, 761–776, https://doi.org/10.1046/j.1365-2427.2002.00905.x, 2002.

Andrew William McCoy: Numerical investigations using LES: exploring flow physics and mass exchange processes near groynes, University of Iowa, https://doi.org/10.17077/etd.vt63cy20, 2006.

Brookes, A.: Traditional engineering methods, physical consequences and alternative practices, Progress in Physical Geography: Earth and Environment, 9, 44–73, https://doi.org/10.1177/030913338500900103, 1985.

Arnaud, F.: Approches géomorphologiques historique et expérimentale pour la restauration de la dynamique sédimentaire d'un tronçon fluvial aménagé: le cas du Vieux Rhin entre Kembs et Breisach (France, Allemagne), PhD thesis, Université Lumière Lyon 2, Lyon, France, 2012.

Arnaud, F., Piégay, H., Schmitt, L., Rollet, A. J., Ferrier, V., and Béal, D.: Historical geomorphic analysis (1932–2011) of a by-passed river reach in process-based restoration perspectives: the Old Rhine downstream of the Kembs diversion dam (France, Germany), Geomorphology, 236, 163–177, https://doi.org/10.1016/j.geomorph.2015.02.009, 2015.

Arnaud, F., Schmitt, L., Johnstone, K., Rollet, A.-J., and Piégay, H.: Engineering impacts on the Upper Rhine channel and floodplain over two centuries, Geomorphology, 330, 13–27, https://doi.org/10.1016/j.geomorph.2019.01.004, 2019.

Arnaud, F., Sehen Chanu, L., Grillot, J., Riquier, J., Piégay, H., Roux-Michollet, D., Carrel, G., and Olivier, J.-M.: Historical cartographic and topo-bathymetric database on the French Rhône River (17th–20th century), Earth System Science Data, 13, 1939–1955, https://doi.org/10.5194/essd-13-1939-2021, 2021.

Belletti, B., Garcia de Leaniz, C., Jones, J., Bizzi, S., Börger, L., Segura, G., Castelletti, A., van de Bund, W., Aarestrup, K., Barry, J., Belka, K., Berkhuysen, A., Birnie-Gauvin, K., Bussettini, M., Carolli, M., Consuegra, S., Dopico, E., Feierfeil, T., Fernández, S., Fernandez Garrido, P., Garcia-Vazquez, E., Garrido, S., Giannico, G., Gough, P., Jepsen, N., Jones, P. E., Kemp, P., Kerr, J., King, J., Łapińska, M., Lázaro, G., Lucas, M. C., Marcello, L., Martin, P., McGinnity, P., O'Hanley, J., Olivo del Amo, R., Parasiewicz, P., Pusch, M., Rincon, G., Rodriguez, C., Royte, J., Schneider, C. T., Tummers, J. S., Vallesi, S., Vowles, A., Verspoor, E., Wanningen, H., Wantzen, K. M., Wildman, L., and Zalewski, M.: More than one million barriers fragment Europe's rivers, Nature, 588, 436–441, https://doi.org/10.1038/s41586-020-3005-2, 2020.

Bravard, J.-P.: Discontinuities in braided patterns: the River Rhône from Geneva to the Camargue delta before river training, Geomorphology, 117, 219–233, https://doi.org/10.1016/j.geomorph.2009.01.020, 2010.

Bravard, J.-P., and Petts, G. E.: Human impacts on fluvial hydrosystems, in: The Fluvial Hydrosystems, edited by Petts, G. E. and Amoros, C., Springer, Dordrecht, 242–262, https://doi.org/10.1007/978-94-009-1491-9_11, 1996.

Brenna, A., Bizzi, S., and Surian, N.: A width-based approach to estimating historical changes in coarse sediment fluxes at river reach and network scales, Earth Surface Processes and Landforms, 47, 2560–2579, https://doi.org/10.1002/esp.5395, 2022.

Brenna, A., Bizzi, S., and Surian, N.: How multiple anthropic pressures may lead to unplanned channel patterns: insights from the evolutionary trajectory of the Po River (Italy), CATENA, 234, 107598, https://doi.org/10.1016/j.catena.2023.107598, 2024.

Brooker, M. P.: The ecological effects of channelization, The Geographical Journal, 151, 63–69, https://doi.org/10.2307/633280, 1985.

Bryant, R. G., and Gilvear, D. J.: Quantifying geomorphic and riparian land cover changes either side of a large flood event using airborne remote sensing: River Tay, Scotland, Geomorphology, 29, 307–321, https://doi.org/10.1016/S0169-555X(99)00023-9, 1999.

Citterio, A., and Piégay, H.: Overbank sedimentation rates in former channel lakes: characterization and control factors, Sedimentology, 56, 461–482, https://doi.org/10.1111/j.1365-3091.2008.00979.x, 2009.

Copeland, R. R.: Bank protection techniques using spur dikes, U.S. Army Engineer Waterways Experiment Station, 1983.

Crutzen, P. J., and Stoermer, E. F.: The Anthropocene (2000), in: Paul J. Crutzen and the Anthropocene: A New Epoch in Earth's History, edited by Benner, S., Lax, G., Crutzen, P. J., Pöschl, U., Lelieveld, J., and Brauch, H. G., Springer, Cham, 19–21, https://doi.org/10.1007/978-3-030-82202-6_2, 2021.

Dépret, T., Riquier, J., and Piégay, H.: Evolution of abandoned channels: insights on controlling factors in a multi-pressure river system, Geomorphology, 294, 99–118, https://doi.org/10.1016/j.geomorph.2017.01.036, 2017.

Downs, P. W., and Piégay, H.: Catchment-scale cumulative impact of human activities on river channels in the late Anthropocene: implications, limitations, prospect, Geomorphology, 338, 88–104, https://doi.org/10.1016/j.geomorph.2019.03.021, 2019.

Dufour, S.: Provansal et al., Geomorphology, https://doi.org/10.1016/j.geomorph.2014.04.033, 2014.

Dynesius, M., and Nilsson, C.: Fragmentation and flow regulation of river systems in the northern third of the world, Science, 266, 753–762, https://doi.org/10.1126/science.266.5186.753, 1994.

Džubáková, K., Piégay, H., Riquier, J., and Trizna, M.: Multi-scale assessment of overflow-driven lateral connectivity in floodplain and backwater channels using LiDAR imagery, Hydrological Processes, 29, 2315–2330, https://doi.org/10.1002/hyp.10361, 2015.

Fryirs, K. A., and Brierley, G. J.: Geomorphic analysis of river systems: an approach to reading the landscape, in: Geomorphic Analysis of River Systems: An Approach to Reading the Landscape, John Wiley & Sons, Chichester, UK; Hoboken, NJ, 1–8, https://doi.org/10.1002/9781118305454.ch1, 2012.

Geerling, G. W., Ragas, A. M. J., Leuven, R. S. E. W., van den Berg, J. H., Breedveld, M., Liefhebber, D., and Smits, A. J. M.: Succession and rejuvenation in floodplains along the River Allier (France), Hydrobiologia, 565, 71–86, https://doi.org/10.1007/s10750-005-1906-6, 2006.

Gilvear, D., and Bryant, R.: Analysis of aerial photography and other remotely sensed data, 135–170, https://doi.org/10.1002/0470868333.ch6, 2005.

Graf, W. L.: The rate law in fluvial geomorphology, American Journal of Science, 277, https://doi.org/10.2475/ajs.277.2.178, 1977.

Gregory, K. J.: The human role in changing river channels, Geomorphology, 79, 172–191, https://doi.org/10.1016/j.geomorph.2006.06.018, 2006.

https://doi.org/10.5194/egusphere-2026-3582
Preprint. Discussion started: 10 July 2026

Gurnell, A. M.: Channel change on the River Dee meanders, 1946–1992, from the analysis of air photographs, Regulated Rivers: Research & Management, 13, 13–26, https://doi.org/10.1002/(SICI)1099-1646(199701)13:1<13::AID-RRR420>3.0.CO;2-W, 1997.

Habersack, H., Hein, T., Stanica, A., Liska, I., Mair, R., Jäger, E., Hauer, C., and Bradley, C.: Challenges of river basin management: current status of, and prospects for, the River Danube from a river engineering perspective, Science of The Total Environment, 543, 828–845, https://doi.org/10.1016/j.scitotenv.2015.10.123, 2016.

Haschenburger, J. K., and Cowie, M.: Floodplain stages in the braided Ngaruroro River, New Zealand, Geomorphology, 103, 466–475, https://doi.org/10.1016/j.geomorph.2008.07.016, 2009.

Hohensinner, S., Habersack, H., Jungwirth, M., and Zauner, G.: Reconstruction of the characteristics of a natural alluvial river–floodplain system and hydromorphological changes following human modifications: the Danube River (1812–1991), River Research and Applications, 20, 25–41, https://doi.org/10.1002/rra.719, 2004.

Hudson, P. F., Middelkoop, H., and Stouthamer, E.: Flood management along the Lower Mississippi and Rhine Rivers (the Netherlands) and the continuum of geomorphic adjustment, Geomorphology, 101, 209–236, https://doi.org/10.1016/j.geomorph.2008.07.001, 2008.

Ibisate, A., Díaz, E., Ollero, A., Acín, V., and Granado, D.: Channel response to multiple damming in a meandering river, middle and lower Aragón River (Spain), Hydrobiologia, 712, 5–23, https://doi.org/10.1007/s10750-013-1490-0, 2013.

Janssen, P., Stella, J. C., Räpple, B., Gruel, C.-R., Seignemartin, G., Pont, B., Dufour, S., and Piégay, H.: Long-term river management legacies strongly alter riparian forest attributes and constrain restoration strategies along a large, multi-use river, Journal of Environmental Management, 279, 111630, https://doi.org/10.1016/j.jenvman.2020.111630, 2021.

Kelly, J. M., Scarpino, P., Berry, H., Syvitski, J., and Meybeck, M.: Rivers of the Anthropocene, University of California Press, https://doi.org/10.1525/luminos.43, 2017.

Kondolf, G. M.: Profile: Hungry Water: Effects of Dams and Gravel Mining on River Channels, Environmental Management, 21, 533–551, https://doi.org/10.1007/s002679900048, 1997.

Laval, F.: Étude préalable à la réalisation du schéma directeur de gestion sédimentaire du Rhône. Rapport de synthèse, https://doi.org/10.13140/RG.2.2.18565.67044, 2022.

Liébault, F., and Piégay, H.: Causes of 20th century channel narrowing in mountain and piedmont rivers of southeastern France, Earth Surface Processes and Landforms, 27, 425–444, https://doi.org/10.1002/esp.328, 2002.

Middelkoop, H., and Van der Perk, M.: Modelling spatial patterns of overbank sedimentation on embanked floodplains, Geografiska Annaler: Series A, Physical Geography, 80, 95–109, https://doi.org/10.1111/j.0435-3676.1998.00029.x, 1998.

Nilsson, C., and Berggren, K.: Alteration of riparian ecosystems caused by river regulation, BioScience, 50, 783–792, https://doi.org/10.1641/0006-3568(2000)050[0783:AORECB]2.0.CO;2, 2000.

Olivier, J.-M., Dole-Olivier, M.-J., Amoros, C., Carrel, G., Malard, F., Lamouroux, N., and Bravard, J.-P.: Chapter 7 – The Rhône River Basin, in: Rivers of Europe, Academic Press, London, 247–295, https://doi.org/10.1016/B978-0-12-369449-2.00007-2, 2009.

Olivier, J.-M., Carrel, G., Lamouroux, N., Dole-Olivier, M.-J., Malard, F., Bravard, J.-P., Piégay, H., Castella, E., and Barthélemy, C.: Chapter 11 – The Rhône River Basin, in: Rivers of Europe (2nd ed.), Elsevier, 393–453, https://doi.org/10.1016/B978-0-08-102612-0.00011-0, 2022.

Bonneuil, C., and Fressoz, J.-B.: L'Événement Anthropocène, la Terre, l'histoire et nous, Le Seuil, Paris, 304 pp., 2014.

Parrot, E: Analyse spatio-temporelle de la morphologie du chenal du Rhône du Léman à la Méditerranée, PhD thesis, Université Jean Moulin Lyon 3, 2015.

Petit, F., Poinsart, D., and Bravard, J.-P.: Channel incision, gravel mining and bedload transport in the Rhône river upstream of Lyon, France ("canal de Miribel"), CATENA, 26, 209–226, https://doi.org/10.1016/0341-8162(95)00047-X, 1996.

Petts, G. E., and Amoros, C.: The fluvial hydrosystem, in: The Fluvial Hydrosystems, edited by Petts, G. E. and Amoros, C., Springer, Dordrecht, 1–12, https://doi.org/10.1007/978-94-009-1491-9_1, 1996.

Petts, G. E., and Gurnell, A. M.: Dams and geomorphology: research progress and future directions, Geomorphology, 71, 27–47, https://doi.org/10.1016/j.geomorph.2004.02.015, 2005.

Piégay, H., and Schumm, S. A.: System approaches in fluvial geomorphology, in: Tools in Fluvial Geomorphology, John Wiley & Sons, 103–134, https://doi.org/10.1002/0470868333.ch5, 2003.

Przedwojski, B.: Bed topography and local scour in rivers with banks protected by groynes, Journal of Hydraulic Research, 33, 257–273, https://doi.org/10.1080/00221689509498674, 1995.

Räpple, B.: Patrons de sédimentation et caractéristiques de la ripisylve dans les casiers Girardon du Rhône: approche comparative pour une analyse des facteurs de contrôle et une évaluation des potentialités écologiques, PhD thesis, Université de Lyon, Lyon, France, 2018.

Riquier, J., Piégay, H., Lamouroux, N., and Vaudor, L.: Are restored side channels sustainable aquatic habitat features? predicting the potential persistence of side channels as aquatic habitats based on their fine sedimentation dynamics, Geomorphology, 295, 507–528, https://doi.org/10.1016/j.geomorph.2017.08.001, 2017.

Roux, A. L., Bradley, J. B., Amoros, C., and Pautou, G.: Ecological changes of the French Upper Rhône River since 1750, in: Historical change of large alluvial rivers: Western Europe, edited by Petts, G. E., Möller, H., and Roux, A. L., 323–350, 1989.

Scott, M. L., Shafroth, P. B., and Auble, G. T.: Responses of riparian cottonwoods to alluvial water table declines, Environmental Management, 23, 347–358, https://doi.org/10.1007/s002679900191, 1999.

Seignemartin, G., Mourier, B., Riquier, J., Winiarski, T., and Piégay, H.: Dike fields as drivers and witnesses of twentieth-century hydrosedimentary changes in a highly engineered river (Rhône River, France), Geomorphology, 431, 108689, https://doi.org/10.1016/j.geomorph.2023.108689, 2023.

Sukhodolov, A. N., Uijttewaal, W. S. J., and Engelhardt, C.: On the correspondence between morphological and hydrodynamical patterns of groyne fields, Earth Surface Processes and Landforms, 27, 289–305, https://doi.org/10.1002/esp.319, 2002.

Sukhodolov, A. N.: Hydrodynamics of groyne fields in a straight river reach: insight from field experiments, Journal of Hydraulic Research, 52, 105–120, https://doi.org/10.1080/00221686.2014.880859, 2014.

Sukhodolov, A. N., Sukhodolova, T. A., and Krick, J.: Effects of vegetation on turbulent flow structure in groyne fields, Journal of Hydraulic Research, 55, 1–15, https://doi.org/10.1080/00221686.2016.1211183, 2017.

Surian, N., and Rinaldi, M.: Morphological response to river engineering and management in alluvial channels in Italy, Geomorphology, 50, 307–326, https://doi.org/10.1016/S0169-555X(02)00219-2, 2003.

Tena, A., Piégay, H., Seignemartin, G., Barra, A., Berger, J. F., Mourier, B., and Winiarski, T.: Cumulative effects of channel correction and regulation on floodplain terrestrialisation patterns and connectivity, Geomorphology, 354, 107034, https://doi.org/10.1016/j.geomorph.2020.107034, 2020.

Thorel, M., Piégay, H., Barthélémy, C., Räpple, B., Gruel, C.-R., Marmonier, P., Winiarski, T., Bedell, J.-P., Arnaud, F., Roux, G., Stella, J. C., Seignemartin, G., Tena-Pagan, A., Wawrzyniak, V., Roux-Michollet, D., Oursel, B., Fayolle, S., Bertrand, C., and Franquet, E.: Socio-environmental implications of process-based restoration strategies in large rivers: should we remove novel ecosystems along the Rhône (France)?, Reg. Environ. Change, 18, 2019–2031, https://doi.org/10.1007/s10113-018-1325-7, 2018.

Tockner, K., and Stanford, J. A.: Riverine flood plains: present state and future trends, Environmental Conservation, 29, 308–330, https://doi.org/10.1017/S037689290200022X, 2002.

Tockner, K., Pennetzdorfer, D., Reiner, N., Schiemer, F., and Ward, J. V.: Hydrological connectivity and the exchange of organic matter and nutrients in a dynamic river–floodplain system (Danube, Austria), Freshwater Biology, 41, 521–535, https://doi.org/10.1046/j.1365-2427.1999.00399.x, 1999.

Vauclin, S., Mourier, B., Tena, A., Piégay, H., and Winiarski, T.: Effects of river infrastructures on the floodplain sedimentary environment in the Rhône River, Journal of Soils and Sediments, 20, 2697–2708, https://doi.org/10.1007/s11368-019-02449-6, 2020.

Vázquez-Tarrío, D., Tal, M., Camenen, B., and Piégay, H.: Effects of continuous embankments and successive run-of-the-river dams on bedload transport capacities along the Rhône River, France, Science of the Total Environment, 658, 1375–1389, https://doi.org/10.1016/j.scitotenv.2018.12.109, 2019.

Vörösmarty, C. J., Meybeck, M., Fekete, B., Sharma, K., Green, P., and Syvitski, J. P. M.: Anthropogenic sediment retention: major global impact from registered river impoundments, Global and Planetary Change, 39, 169–190, https://doi.org/10.1016/S0921-8181(03)00023-7, 2003.

Winterbottom, S. J.: Medium and short-term channel planform changes on the Rivers Tay and Tummel, Scotland, Geomorphology, 34, 195–208, https://doi.org/10.1016/S0169-555X(00)00007-6, 2000.